CHAPTER 6

RESULTS AND DISCUSSION OF THE OPTICAL PROPERTIES

6.1 The ITO case

6.1.1 Optical transmittance

A systematic study of the laser deposited ITO films was accomplished, to test their possible use as electrodes in DSC applications. As already mentioned in the previous chapter, the nature of the glass substrate is an important parameter as it determines the different properties of the films deposited onto it. For instance for optical transmittance measurements, the ideal substrate should be highly transparent and for Rutherford backscattering spectrometry thickness measurements, the substrate should be either elemental (e.g., Si) or of very simple composition (e.g., SiO_2). In the present work, two kinds of substrate have been used. ITO films were deposited onto silica (SiO_2) fused-quartz glass substrates, while TiO_2 films were first deposited onto silicon (Si) substrates and later onto ITO films to form multilayered thin films. The optical transmittance and reflectance measurements were made using a double beam spectrophotometer Perkin Elmer Lambda 900 in the UV-visible-near IR region. All transmittance and reflectance values were normalised to the values of the bare substrates.

6.1.2 Optical transmittance dependence on the pulse number

Fig.6.1 shows the transmission spectra of the SiO_2 and the Si substrates. The SiO_2 is about 95% transparent in the range 300 to 2400nm, while the Si is only ~ 22% transparent in the IR range (1000-3000nm). The optical transmittance of typical ITO films grown on SiO_2 at room temperature and an oxygen pressure of 1Pa is displayed in Fig.6.2. The ITO films were prepared with different laser pulse numbers as, indicated in the figure, by the ArF (λ=193nm) excimer laser (Lambda Physik, LPX 305 i), operated with a repetition rate of 10Hz and a pulse length of τ=30ns (FWHM). For all the thin films discussed in this chapter, the energy of the

laser and the spot size were adjusted to maintain a fluence of about 4J/cm^2. A high optical transmission, above 88%, has been measured in the visible region for all the films deposited at room temperature, except for the one deposited with 80000 laser pulses. This later pulse number results in a film thickness higher than 1500nm. Its low transmission is probably due to the roughness of the films as well as the multiple collisions between incident light and ITO particulates in the thick films. The different percentage of transmission and the corresponding pulse number are given in Table 6.1.

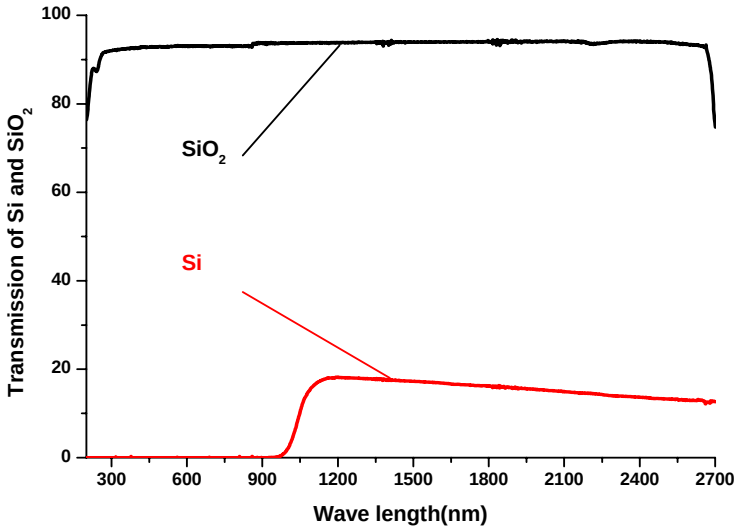

Figure 6.1 Transmission of Si (red curve) and SiO_2 (black curve) substrates.

It can be seen that the transmittance increase as the pulse number decreases. The pulse number determines the thickness of the films: the higher the pulse number, the higher the thickness of the films and the lower the transmission of the light. This is in accordance with the fact that the transmitted quantity of light is affected by the thickness of the film according to the formula

$$I = I_0 \exp(-\alpha d) \tag{6.1}$$

where I is the transmitted light intensity, I_0 is the incident light intensity, d is the thickness and α is the absorption coefficient.

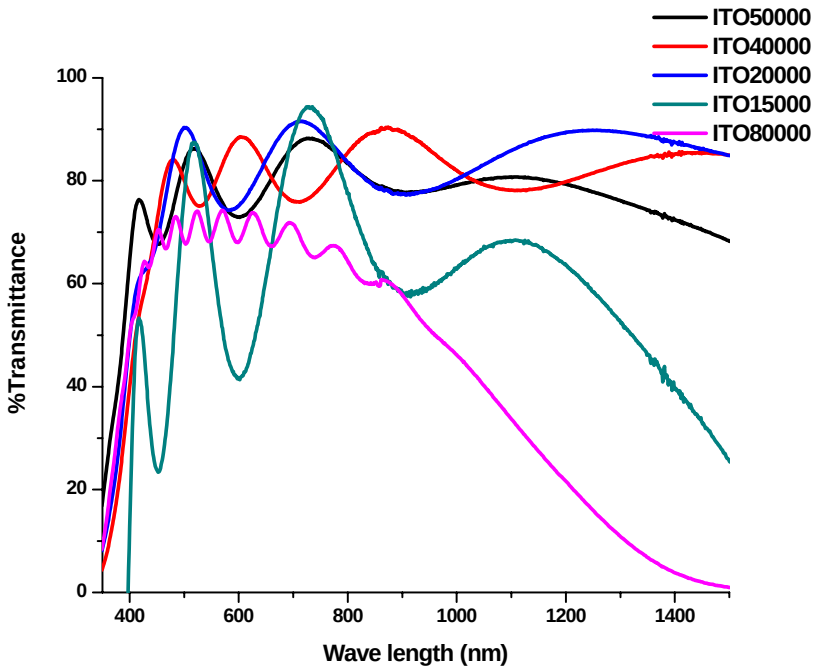

Figure 6.2 Transmittance spectra of ITO films deposited at room temperature with different laser pulse numbers. The transmission is higher where the pulse number is lower.

Table 6.1 Percentage transmission versus pulse number

ITO pulse numbers	Percentage transmission
80000	74.4
50000	88.2
40000	90.3
20000	91.5
15000	96.0

The oscillations in the transmission spectra are caused by optical interference. The behavior of the interference fringes in the transmission spectra proves that the films thickness is very uniform. This is confirmed by measuring the transmission on the same sample but at different edges.

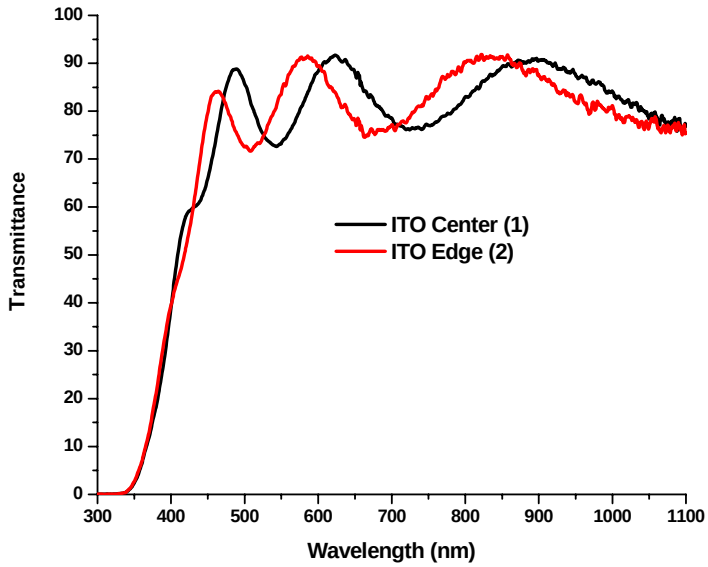

Figure 6.3 Transmittance measurement taken on ITO film deposited at room temperature. The measurement was performed at 2 different points of the sample. 1- at the center, 2- at the corner.

For instance, the Fig.6.3 shows the transmittances taken at the centre and at the edge of one of the film deposited at room temperature and at 1Pa. The uniformity is seen by the percentage transmission for both of the curves (~ 91%) and the behavior of the interference very similar for both graphs.

6.1.3 Optical transmittance dependence on the oxygen pressure and substrate temperature

The optical transmittance as a function of wavelength of the films deposited at room temperature (RT) under different oxygen pressure but same laser pulse number (20000) is shown in Fig.6.4. A high transmittance (above 84%) in the visible-near IR region of the solar spectrum was exhibited by the films prepared under oxygen pressure of 1Pa and above. Lower background pressure resulted in translucent films with dark brown color as already demonstrated in the previous chapter. Depositions of the ITO films were also performed at high temperatures (200 and 400°C) and at different oxygen pressures.

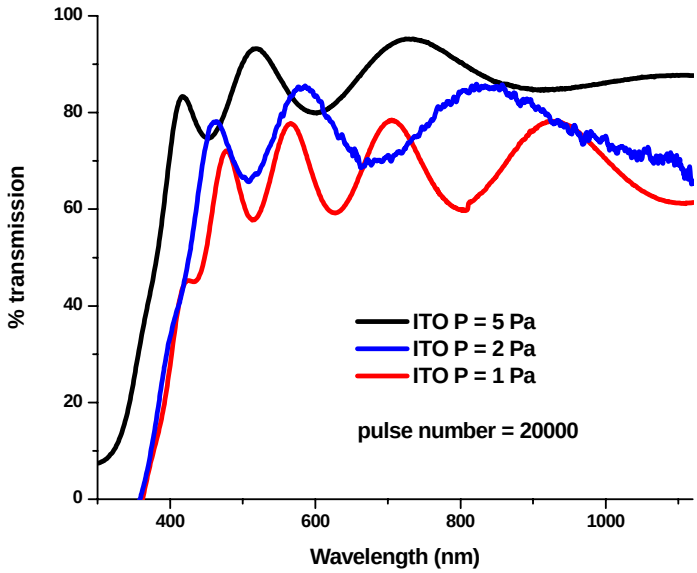

Figure 6.4 Transmission of the ITO films deposited at room temperature and at different oxygen pressure.

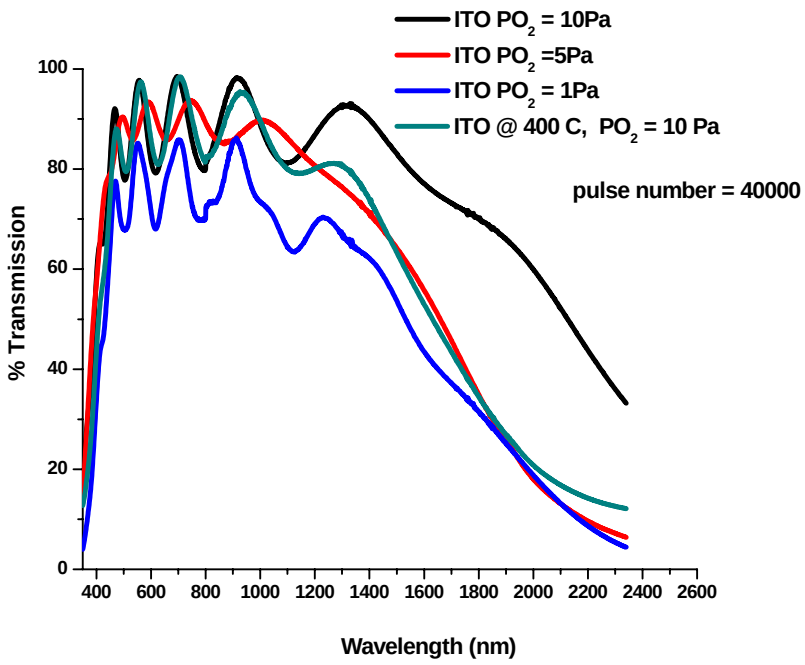

Figure 6.5 Transmission of the ITO films deposited at 200°C and at different oxygen pressure.

Fig.6.5 shows the transmission curve and the corresponding O_2 pressure. Depositions conditions other than temperature and oxygen pressure were maintained constant for each film. Transmittance for ITO deposited at 400°C and 200°C were the same in the Vis region. The transmittance of ITO film deposited at 400°C decreases a little bit near the IR region. The transmittance showed similar characteristics to those of the films prepared at room temperature as regard the increasing of transmittance with increasing of the O_2 pressure. The transmission is about 98% for the films deposited at 10Pa (300nm thick), while it is only 60% for the film deposited at 1Pa, whose thickness results to be a little bit higher (375nm) comparatively to the one deposited at 10Pa with 40000 pulse number.

Table 6.2 resumes the different transmission percentage versus the oxygen pressure for ITO films deposited with the same pulse number (40000). It is important to note that the transmission is somewhat smaller (~ 88%) for the ITO films deposited at room temperature. However, a significant decrease in the near IR transmittance with increasing O_2 pressure was displayed by the films. A high IR reflectance is a desirable feature in window layer coating, especially for application in energy-efficient windows for solar cells [203].

Table 6.2 Percentage transmission versus oxygen pressure of ITO thin films deposited with 40000 pulse number

ITO oxygen pressure (Pa)	Percentage transmission
10	98
5	88
2	80
1	60

From the Fig.6.3 it can be seen that the films deposited at room temperature transmit from 450nm to about 1000nm and more (throughout theVis-NIR region),

whereas the films produced at 200°C exhibit a constant transmission from 400nm (the transmission shifts towards shorter wavelengths) up to 1300nm and more (Vis-NIR). A shift in the absorption edge towards longer wavelengths region with increasing O_2 pressure due to increased free carrier absorption was noticed in the films prepared at room temperature and 200°C. The transmittance in the wavelength range beyond 1300nm for ITO deposited at 1, 5 and 10Pa decreased steeply by the plasma effect due to large carrier concentrations.

The increase in transmittance with the increase of the substrate temperature during deposition can be explained by the fact that the grain size increases significantly with the increasing of temperature, thus reducing the grain boundary scattering. The shift observed is the well known Burstein-Moss shift and is related to the electron density and thus carrier concentration [306-308]. A wider shift to the shorter wavelength region is usually characterised by higher electron density as evidenced in Fig.6.5. These observations are closely correlated with what earlier reported in the literature for ITO and SnO_2 films [206, 309, 310] and will be confirmed by plotting the optical density. This change in the absorption edge (small band-gap widening) is important in window layer coatings, since it can help to prevent unwanted absorption in the luminous spectra range.

It is important to stress that when the thickness is very high (above 1000nm), the transmission decreases very abruptly (around 30%) when the O_2 ambient pressure during the deposition is increased from 1 to 5Pa (Fig.6.6) This is most probably due to the fact that films thick 1000nm and more deposited at lower pressure are deficient in oxygen and, therefore are non stoichiometric films. The increase in the transmission with an increase in oxygen can also be explained by the number of oxygen vacancies in the ITO films. Increasing the oxygen pressure decreases the number of oxygen vacancies in the film and thus decreases the carrier concentration. This decrease leads probably to an improvement of the film crystallinity and increases the film transmission. These data show that the oxygen incorporation into the film is significant at high oxygen pressures, and that the mobility of the atoms on the growing film is more important at high temperature.

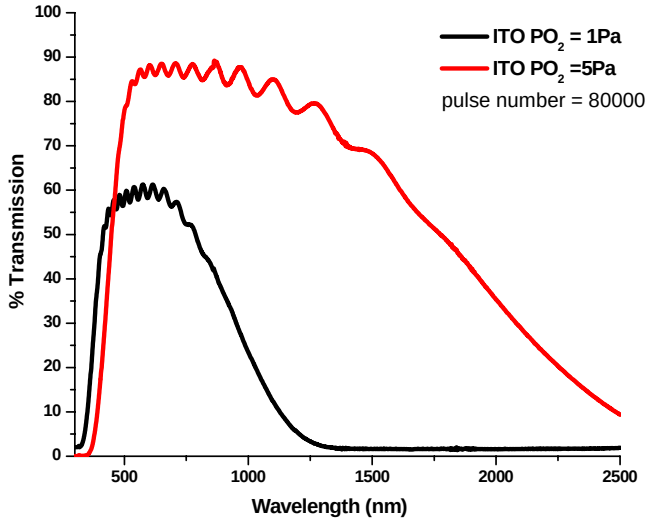

Figure 6.6 Transmission of the ITO films deposited at 200°C and at 5 and 1Pa, a decrease of about 30% transmission is observed.

The data of the transmission through ITO films produced at 200°C in an oxygen atmosphere agree well with other existing data [206, 208, 209]. All the transmittance spectra exhibit interference in the visible and a tail in the IR. This last behavior is probably due to free carrier absorption. The overall trend is that the oxygen background gas is necessary to achieve a high transmission both for films deposited on room and high temperature substrates.

6.1.4 Optical constants

Refractive index, extinction coefficients and thickness of the ITO films were calculated using a home made code [78, 207], in which the measured optical transmission spectra are the main input. The model is suitable for dielectric films deposited onto weakly absorbing substrates (for instance SiO_2) of well known refractive index. The schematic representation of a thin film for calculation of the transmittance T is drawn in Fig.6.7. Basically the theoretical transmission given in the Eq (6.2) is used to model the experimental transmission. The spectrum is divided into 3 different regions, the weakly absorbing region (UV), the transparent region (Visible), and the strongly absorbing region (IR), thus allowing to calculate the refractive index separately. We can write:

$$T = \frac{Ax}{B - Cx\cos\varphi + Dx^2} \tag{6.2}$$

$$A = 16n^2 s,\ B = (n+1)^3(n+s^2),\ C = 2(n^2-1)(n^2-s^2),\ D = (n-1)^3(n-s^2) \tag{6.3}$$

$$\varphi = \frac{4\pi nd}{\lambda},\ x = e^{-\alpha d},\ \alpha = \frac{4\pi k}{\lambda} \tag{6.4}$$

where the parameters A, B, C and D depend on the refractive index n and the extinction coefficient k, d is the thickness of the film and s is the refractive index of the substrate, α represents the absorption coefficient of the film.

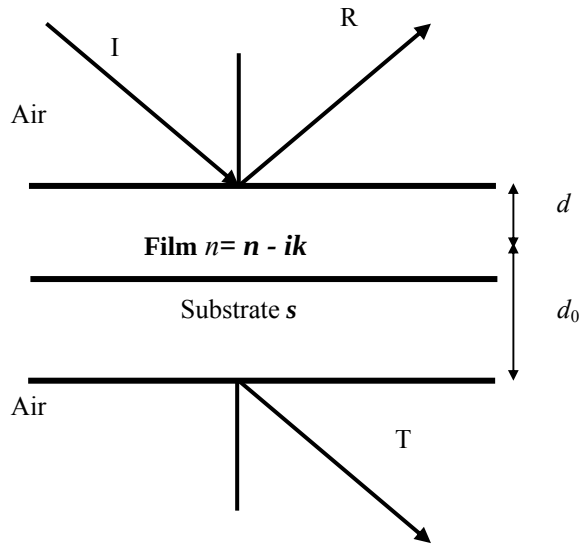

Figure 6.7 Schematic representation of a thin film for calculation of the transmittance T.

Since $-1 < \cos\varphi < 1$, the theoretical transmission values vary between a minimum T_m, for which $\cos\varphi = -1$ and a maximum T_M, for which $\cos\varphi = +1$. Likewise, at the extrema we have $\varphi = 4\pi nd/\lambda = m\pi$, where m is an integer,

$$T_M = \frac{Ax}{B - Cx + Dx^2},\quad \cos\varphi = 1 \tag{6.5}$$

$$T_m = \frac{Ax}{B + Cx + Dx^2},\quad \cos\varphi = -1 \tag{6.6}$$

T_M and T_m are the envelopes of the transmission spectrum tangent to the maxima and minima, respectively. They are calculated by a shape-preserving smooth path line interpolation algorithm [311].

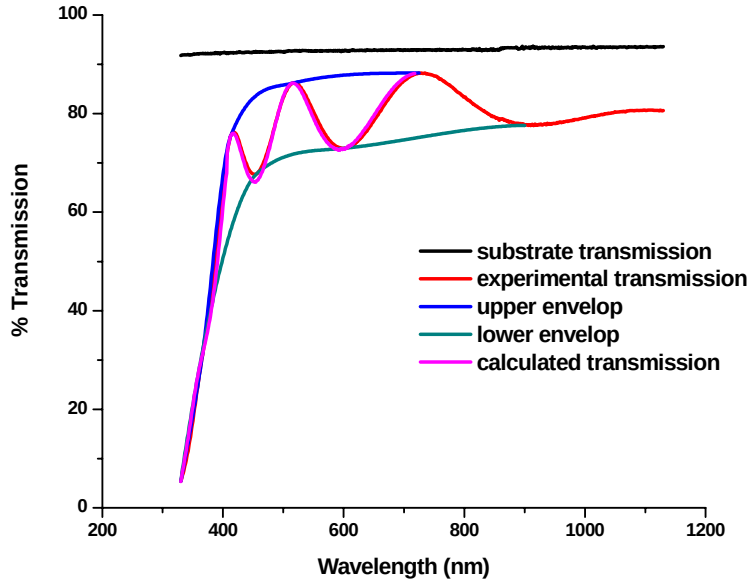

Figure 6.8 Measured and calculated transmittance spectra. The fit between the 2 spectra is regular. The upper (line passing by the maxima) and lower (line passing by the minima) envelopes are really tangent to the extrema. The line at the top shows the transmittance of the substrate.

The refractive index can therefore be calculated knowing the values of the envelopes. Once n is known, the A, B, C and D parameters can be easily evaluated as well as the absorption coefficient α. Fig.6.8 shows an example of the calculated transmission that regularly fits the experimental transmission. When the fitting is done, optical coefficients such as the refractive index and the extinction coefficient of the films can be determined. The refractive index, (Fig.6.9. a), for the films deposited at room temperature and at 1Pa is found to be around 2 through the visible region, close to that in bulk ITO. This means that the stoichiometry is preserved.

The extinction coefficient remains low and almost constant ($6x10^{-3}$) through the

visible region. This feature is a characteristic of a very high transparency of the film in that region. These coefficients are almost the same for all the ITO films deposited at room temperature and at oxygen pressure of 1, 2 and 5Pa. At PO_2=10Pa, there is a decrease of the refractive index from 2.07 to 2.0 (Fig.6.9 b), which is a signal of a change in the stoichiometry of the films. The extinction coefficient in this case is about $3x10^{-4}$, which leads to an increase of the transmission of the solar light.

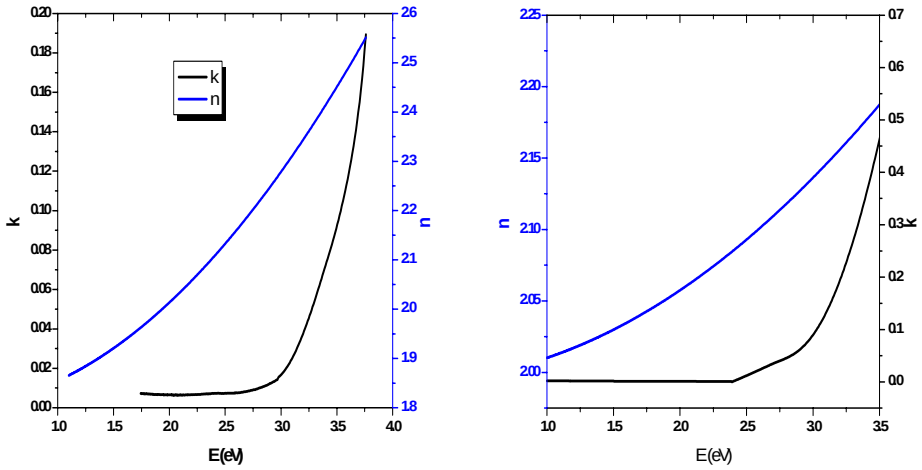

(a) (b)

Figure 6.9 Evaluated refractive index and extinction coefficient of ITO films deposited a) at PO_2=10Pa. b) at PO_2=1Pa. The values are consistent with bulk.

6.1.5 Absorption and energy transition

At shorter wavelengths, close to the optical E_g, scattering losses are dominated by fundamental absorption α which is often expressed as:

$$\alpha = -\ln(T)/d \tag{6.7}$$

where d is the film thickness. From the solid-state band theory, it is known that near the absorption edge, due to direct interband transition, the absorption coefficient, when scattering effects are neglected, can be expressed as a function of the incident photon energy according to the following formula

$$(\alpha h\nu)^2 = \alpha_0 (h\nu - E_g) \tag{6.8}$$

where α is the absorption coefficient, α_0 is a constant having a numerical value $2x10^4$ when α is expressed in cm^{-1} and $h\nu$ and E_g in eV. E_g is the band-gap energy. Direct interband transition is the mode in which light is absorbed in direct band gap semiconductor. Absorption of photon results in an excitation of an electron from the valence band up to the conduction band, leaving a hole in the valence band. In such transition, both energy and momentum must be conserved, a photon has quite a large energy ($h\nu$) but a small momentum h/λ. Because the photon momentum is small compared to the system momentum, the latter ITO is essentially conserved in the transition.

By using Eqs. (6.7) and (6.8) α was calculated as a function of photon energy. It is found that absorption and energy transition are strongly affected by the thickness of the film, the oxygen pressure in the RPLAD chamber during deposition and the temperature of substrates. Fig.6.10 shows the plot of the absorption coefficient for different ITO films deposited at room temperature under different pulse number. The plot is linear in the region of strong absorption near the fundamental absorption edge. Therefore, the absorption takes place through direct transition and the extrapolation of the transition linear region on the photon energy-axis using Tauc's plot [312] gives the value of the nearly direct band gap E_g.

In Fig.6.10, the absorption is observed to be proportional to the thickness of the ITO films. The band gap is approximately 3.75eV for films deposited with 80000 pulse numbers and 3.43eV for films deposited with 20000 pulse number. These values are coherent, since indium tin oxide is commonly referred as an n-type semiconductor with a large band gap between 3.5 and 4.3eV. The experimental values agree well with those quoted in the literature [313, 314]. The shift observed in the direct band gap, although not very significant, can be attributed to the different thickness of the films (due to the different laser pulse numbers).

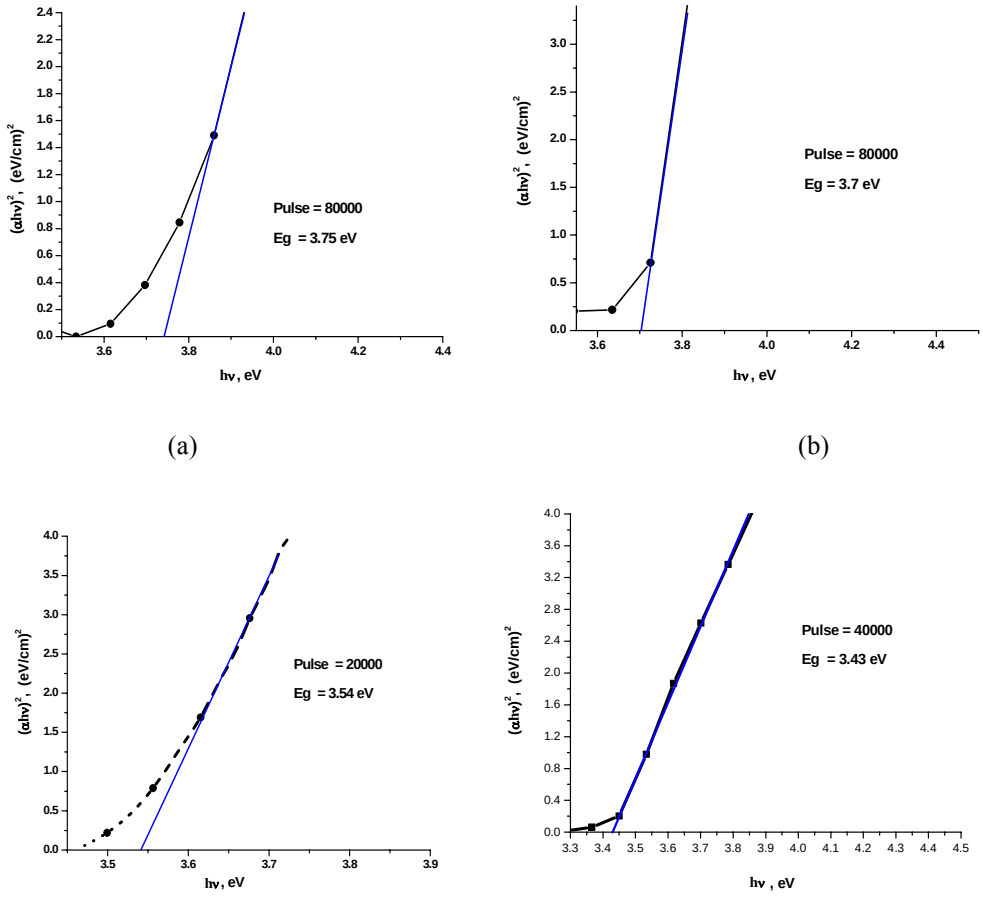

Figure 6.10 Plots of $(\alpha h\nu)^2$ versus hν for ITO films deposited at room temperature with different pulse numbers.

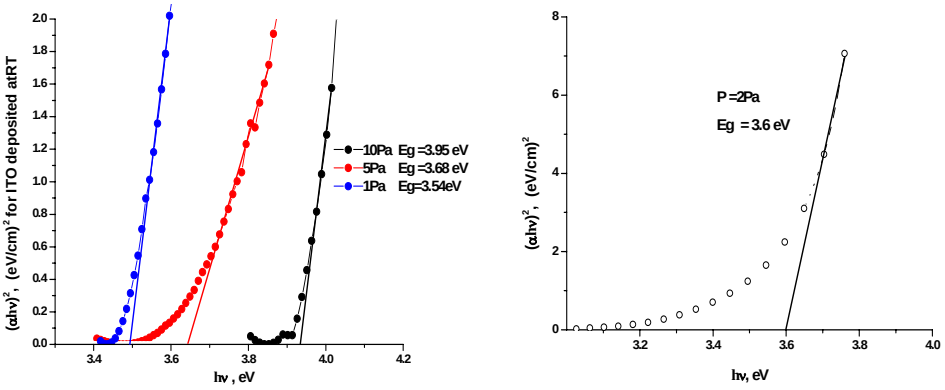

Figure 6.11 Plots of $(\alpha h\nu)^2$ vs (hν) of ITO films deposited at different O_2 pressure; the extrapolation of the straight line of the curve gives the value of the transition energy E_g.

Fig.6.11 shows the variation of $(\alpha h\nu)^2$ versus hν for ITO deposited at 200°C and at different O_2 pressure at constant pulse number (40000). The O_2 pressure also affects the direct band gap. The direct band gap of the ITO films increases from 3.54eV to 3. 95eV when the O_2 pressure increases from 1Pa to 10Pa. This increase in the direct band gap with an increase in oxygen pressure is due to a decrease in carrier concentration. This is also explained by the Burstein-Moss shift [309, 310], which is related to the carrier concentration in the film.

In Fig.6.12 the variation of $(\alpha h\nu)^2$ vs (hν) for ITO films deposited at room temperature and at 200°C is shown. As the carrier concentration increases with the increase of the substrate temperature, the direct band gap increases from 3.6eV at room temperature to 3.75eV at 200°C. As the photon energy increases, so does the value of the thin film momentum at which the transition occurs.

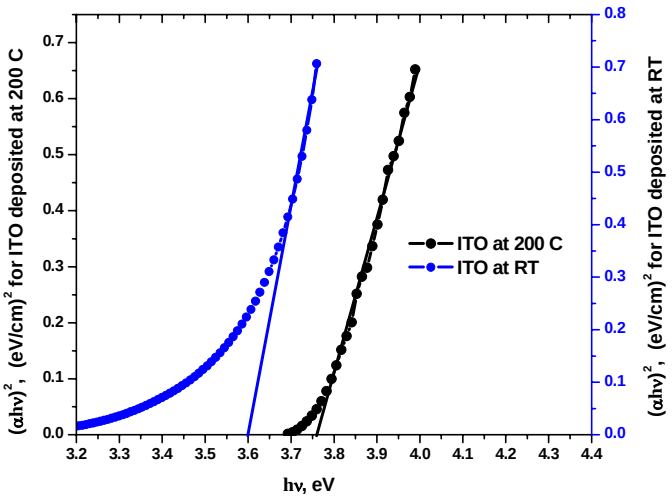

Figure 6.12 Plots of $(\alpha h\nu)^2$ vs (hν) spectra of ITO films deposited at room temperature and at 200°C.

The energy away from the band edge also increases. The probability of absorption depends on the density of the electrons at the energy corresponding to the initial state (before absorption) as well as the density of the empty states at the final energy (after absorption). Since both of these energies increase with energy away from the band edge, a logical consequence is that the absorption coefficient

increases rapidly with increase of photon energy just above E_g. Since the light intensity drops to 1/e of its initial value in passing a distance $1/\alpha$ through the thin film, Eq. (6.7) shows that photon of energy $h\nu \geq E_g$ is absorbed within the first few microns beyond the film surface.

6.2 The TiO_2 case

The TiO_2 thin films submitted to visual inspection were completely transparent, independently of whether they were deposited at room temperature or on heated substrates. From the transmittance spectra, the film thickness values were also determined with the aid of the interference fringes method [296]. Thickness values of about 300nm were found. Similar thickness values were obtained from RBS measurements.

6.2.1 Optical transmittance

In the framework of this research studies, TiO_2 films were deposited on Si substrate for optical and structural characterisation. This work was done in order to study the properties of single layer of TiO_2 and to compare it with multilayers of TiO_2 deposited on the ITO pre-deposited thin film. Fig.6.13 shows the transmission spectra (1000-2500nm) of TiO_2 thin films deposited on the the Si substrates at room temperature, 200°C and 400°C.

Depositions were performed by using the ArF (λ=193nm) excimer laser (Lambda Physik, LPX 305 i), operated at a repetition rate of 10Hz and a pulse length of τ=30ns (FWHM). For all the oxide thin films, the energy of the laser and the spot size were adjusted to maintain a fluence of approximately 4J/cm^2. Films were deposited under different substrates temperatures under oxygen pressure of 10Pa. Under the same deposition conditions, TiO_2 films were also grown on quartz SiO_2 substrates.

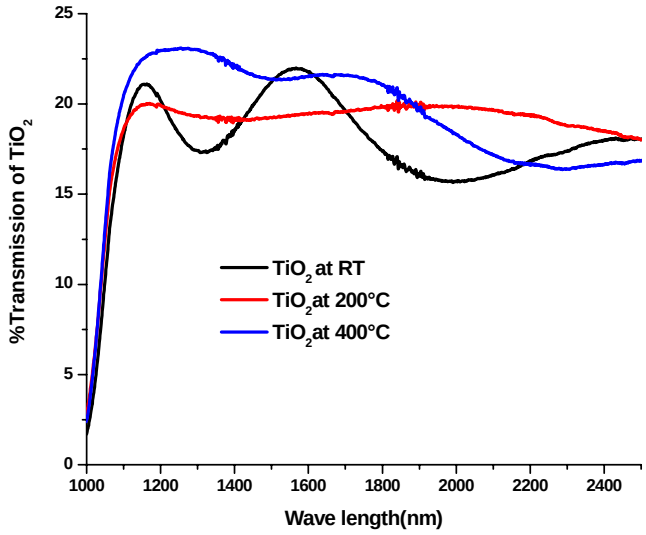

Figure 6.13 Transmission of TiO_2 films deposited on Si at room temperature (black curve), at 200°C (red curve) and at 400°C (blue curve).

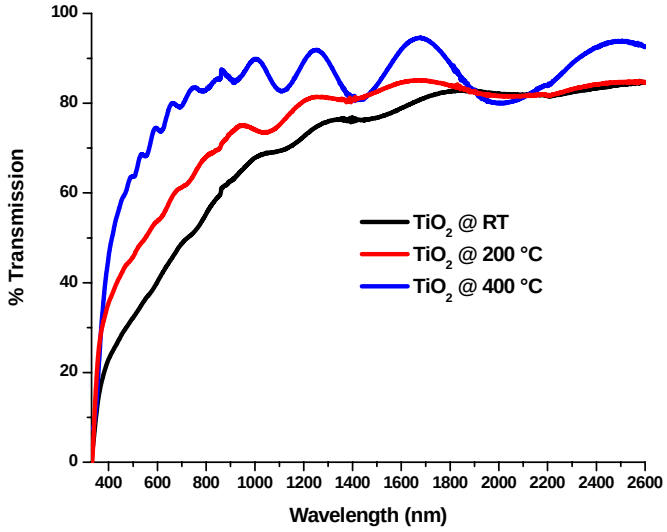

Figure 6.14 Transmission of TiO_2 films deposited on quartz SiO_2 substrates at room temperature, 200°C and at 400°C.

The transmittance spectra of the TiO_2 films deposited at room temperature, 200°C and 400°C substrate temperatures in the UV-Vis-near IR region are can be seen in Fig.6.14. Measurements were made using a double beam spectrophotometer Perkin Elmer Lambda 900 in the UV-visible-near IR region. As in the case of ITO

thin film transmittance measurements, the wave pattern is attributed to the light interference. It can be observe that the number of interference peaks increased with the thickness of the film. The sharp decrease in transparency of the thin films, in the IR region, for deposition done on Si, and in the UV-Vis region for deposition done on quartz SiO_2, respectively results from the fundamental light absorption of the semiconductor. For both type of substrates, the best transmission is obtained for TiO_2 thin films deposited at 400°C.

A transmission higher that 92% in the Vis-NIR region has been obtained for TiO_2 deposited on quartz SiO_2 substrates, while it is only ~20% in IR region for the films deposited on Si. However, in the case of TiO_2 thin films deposited on Si at higher temperature, the transmission is practically the same as that of the bare substrate. The average transmission value of the TiO_2 films are higher than those reported for tetragonal anatase phase TiO_2 films, obtained recently by other deposition techniques [315-316] or even by the RPLAD of Ti thin films followed by thermal oxidation in an O_2 atmosphere [317]. The absorption edge of the TiO_2 films deposited at high temperatures (200°C and 400°C) is observed at a higher wavelength range than that of the TiO_2 films deposited at room temperature.

The shift is ascribed to the difference in grain size as thin films which underwent a short-term heat treatment contained relatively small crystallites. The energy of the particles impinging on the substrate is taken as parameter to define regions where rutile, anatase and amorphous TiO_2 films can be expected [318]. For particles with energies in the range 1-10eV, the energy of particle impacts influences the atoms in their near vicinity. Momentum transfer from impinging particles to growing TiO_2 films is considered to cause nucleation of “crystalline” phases. In order to rearrange adsorbed particles at low temperatures, the impinging particle needs to have enough kinetic energy to exceed the specific potential barrier for crystallisation. This corresponds to the crystalline nucleation energy of TiO_2.

From a microscopic point of view, these observations are also considered to correlate with both the fundamental optical absorption edge characteristics and the

phase composition in TiO_2 films. When the TiO_2 thin film deposited at 400°C is further annealed at 300°C and 500°C for 3 consecutive hours, the transmission decreases considerably throughout the UV-Vis-NIR with the annealing temperature (Fig.6.15). The decrease in transmittance is most significant at the shorter wavelengths. This decrease in transparency in the visible region results fundamentally in a light absorption due to a change in a crystalline phase. It can also be explained in terms of the Burstein-Moss effect as the conduction band is pushed to higher energies by the increase in carrier concentration.

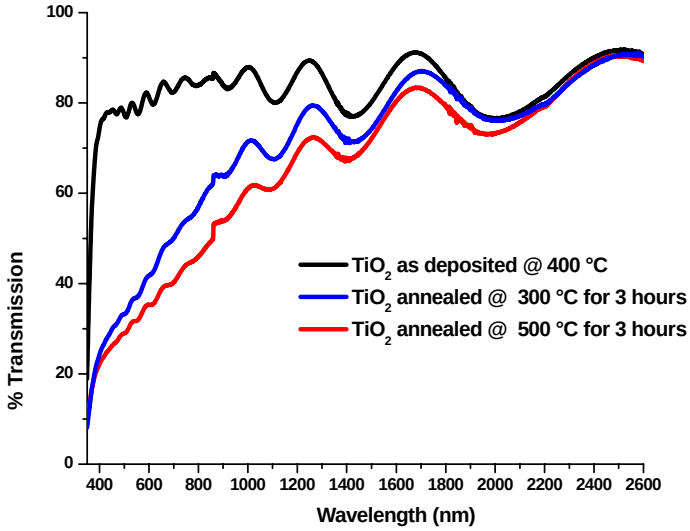

Figure 6.15 Transmission of TiO_2 films, as deposited on quartz SiO_2 at 400°C and annealed after deposition at 300°C and 400°C for 3 consecutive hours.

6.2.2 Refractive index

Fig.6.16 shows the wavelength dependence of the refractive index (n) for a TiO_2 films deposited on Si and quartz SiO_2 at 400°C, while in Fig.6.17 the refractive index dependence on the wavelength (nm) is shown for the TiO_2 films annealed at 300°C and 500°C for 3 consecutive hours. The refractive index decreases as the wavelength increases. At long wavelength (above 600nm) there is no dispersion and the value of the refractive index varies very little. At short wavelength there is a high dispersion leading to an increase of the refractive index increases abruptly.

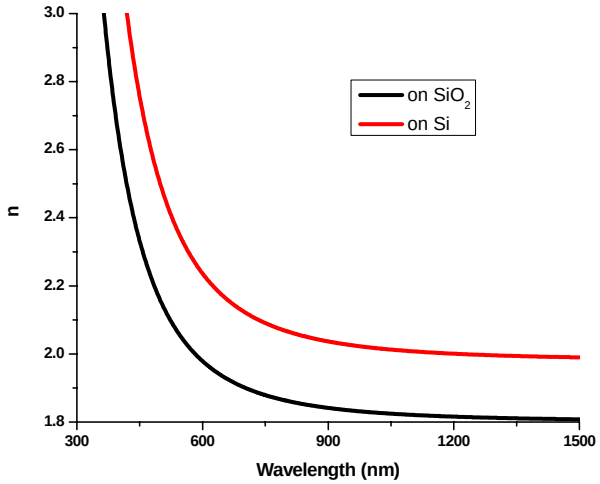

Figure 6.16 Wavelength dependence of the refractive index for a TiO_2 films deposited on Si and quartz SiO_2 at 400°C.

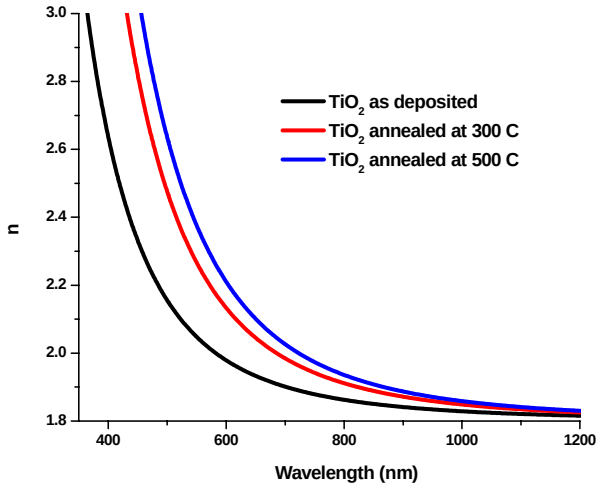

Figure 6.17 Wavelength dependence of the refractive index for a TiO_2 films deposited on quartz SiO_2 at 400°C, and annealed at 300°C and 500°C for 3 consecutive hours.

A high value of the refractive index measured at 550nm was 2.33 for the TiO_2 deposited on Si and 2.04 for TiO_2 deposited in quartz SiO_2. The refractive index of the TiO_2 films deposited on Si is higher than that for TiO_2 deposited on quartz SiO_2. The increase of the refractive index is attributed to the crystalline structure

of the substrate, since the Si was <111> oriented while the quartz SiO_2 substrate was amorphous. The refractive index of the TiO_2 films deposited on quartz SiO_2 at 400°C increases with the post-annealing temperature: the value of n at 550nm was 2.26 for films annealed at 300°C and 2.37 for films annealed at 500°C.

It is important to notice that the refractive index of TiO_2, annealed at 500°C for 3 hours is close to that of anatase phase TiO_2. Values close to this one have been reported elsewhere [319, 320]. As already noticed above, the dispersion is more intense at short wavelength than at high wavelength (near IR and above). The annealing seems not to affect the refractive index of the TiO_2 films. Since annealing of the films brings modification in structure, rendering the films more crystalline, one can deduce that the refractive index of TiO_2 films is strongly affected by the crystal phase of the films, the crystalline size and the density of the films. These remarks have been evidenced by Brinker et al. [314], who reported a reciprocal relationship between the refractive index and the cluster size in silica sol prior to film deposition. They also reported that the higher refractive index of quartz SiO_2 films stems from a smaller degree of porosity.

6.2.3 Optical transmittance of multilayers TiO_2/Au and ITO/TiO_2/Au

The transmission of TiO_2/Au films is shown in Fig.6.18. TiO_2 was deposited on quartz SiO_2 at 400°C and annealed at 300°C and 500°C for 3 consecutive hours, while 500 laser pulses directed on an Au target produced some Au particles deposition on the layer at room temperature. As compared with the transmission curve plotted in Fig.6.15, there is a decrease of about 6% of the transmission in the UV-Vis range. This decrease is attributed to the Au layer deposited on top of the TiO_2 thin films: the Au might have absorbed a part of light since in nanoparticles form its plasmon resonance lies in the visible region.

TiO_2 thin films were deposited on the ITO thin films that were earlier deposited at 200°C. The TiO_2 films were deposited at 200°C and at 400°C with 40000 laser pulses at a oxygen pressure of 10Pa. The TiO_2 was deposited on top of the ITO

films so that only a part of the ITO film surface is covered by the TiO_2 film. To this end, a mask has been designed to protect the remaining ITO film that should not be contaminated by the TiO_2 film. On top of the as deposited TiO_2 film a sub-monolayer of Au was deposited with 500 laser pulses directed to the Au target.

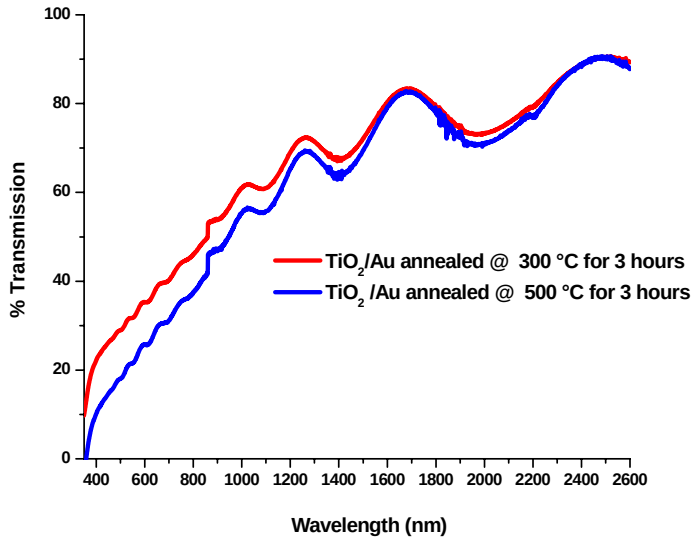

Figure 6.18 Transmission of TiO_2/Au films. TiO_2 was deposited on SiO_2 at 400°C and annealed at 300°C and 500°C for 3 consecutive hours, while a few pulses of Au were deposited at room temperature.

Au was deposited at room temperature with a fluence ($3J/cm^2$) somehow lower than that of the ITO and TiO_2 deposition. The transmission measurements of these deposited multilayers, performed throughout the UV-Vis-near IR range, are shown in Fig.6.19 for the TiO_2 films deposited at 200°C and in Fig.6.20 for the TiO_2 films deposited at 400°C. The transmittance percentage values for each film are given in Table 6.3. The transmission of the ITO/TiO_2 bilayer, where the TiO_2 thin film is deposited at 400°C, is higher than that of the bilayer ITO/TiO_2, where the TiO_2 thin film is deposited at 200°C. This is in accordance with the transmission of the single layer TiO_2 thin film plotted in Fig.6.14. In both cases, the transmission of the bilayer ITO/TiO_2 is higher the one of the single layer ITO thin film. The transmission decreases of about 10% when Au is deposited on the TiO_2 layer.

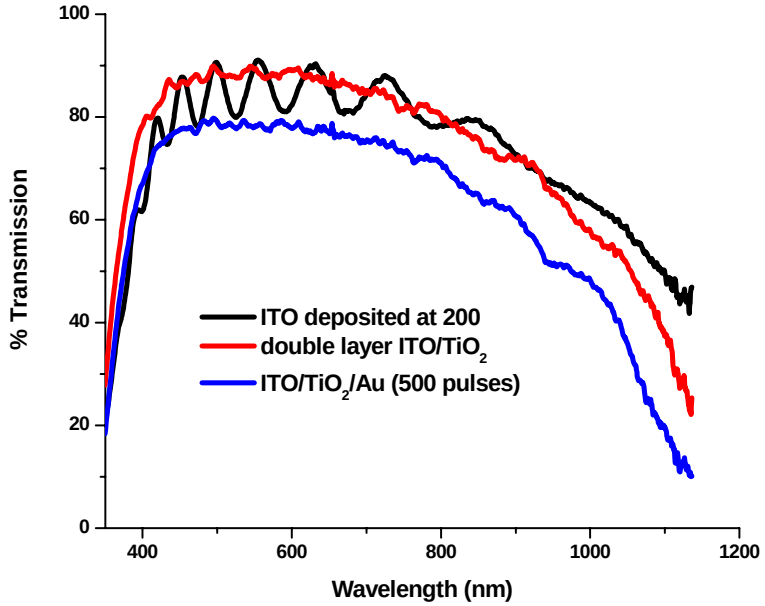

Figure 6.19 Transmission spectra of multilayer ITO/TiO_2/Au (500 pulses). The ITO thin film is deposited on quartz SiO_2 at 200°C and the TiO_2 thin film is deposited on the ITO at the same temperature.

Table 6.3 Percentage transmission of ITO, multilayer ITO/TiO_2 and ITO/TiO_2/Au thin films.

Films (ITO films are deposited at 200°C for the samples)	Percentage transmission (%)	Wavelength range (nm)
ITO	~ 90	415-830
ITO/TiO_2 (TiO_2 deposited at 200°C)	~ 89	400-900
ITO/TiO_2/Au (TiO_2 deposited at 200°C)	~ 79	400-900
ITO/TiO_2 (TiO_2 deposited at 400°C)	~ 93	400-1100
ITO/TiO_2/Au (TiO_2 deposited at 400°C; Au is deposited at room temperature)	~ 83	400-1100

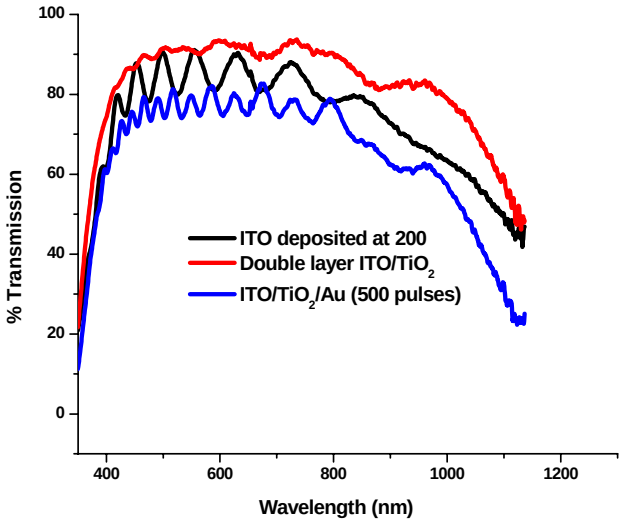

Figure 6.20 Transmission of multilayer ITO/TiO_2/Au (500 pulses). The ITO thin film is deposited on quartz SiO_2 at 200°C, while the TiO_2 thin film is deposited onto the ITO at 400°C.

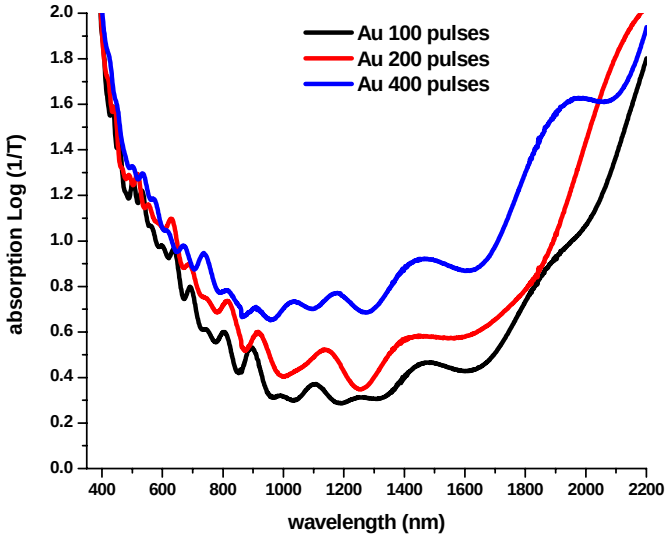

Figure 6.21 Absorption curves of ITO/TiO_2/Au multilayers deposited on quartz SiO_2. Au was deposited with 100, 200 and 400 laser pulses.

This is an indication that there might be absorption of the light intensity produced by the effect of Au deposited on TiO_2 film. This can be confirmed by plotting the absorption spectra of the films (Fig.6.21). Indeed, the spectra show that the

absorption increases with the amount of Au deposited onto the TiO_2 film. To better observe the effect of Au deposited on ITO/TiO_2 bilayers, another series of depositions was performed, where the ITO and TiO_2 thin films were deposited at 200 and 400°C, respectively, and Au was deposited with 100, 200 and 400 laser pulses.

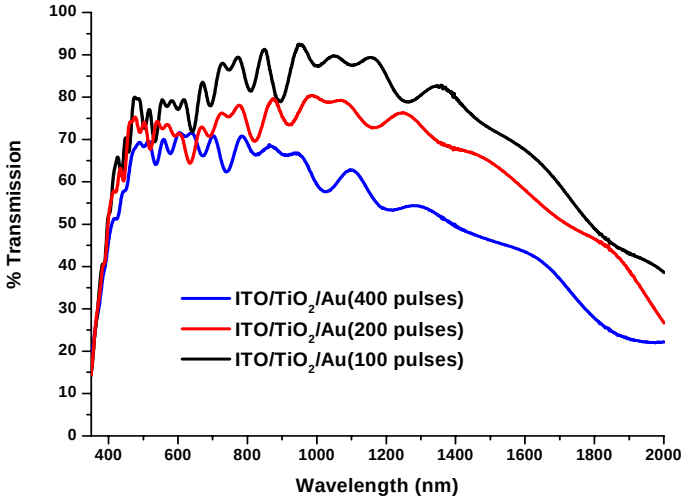

Figure 6.22 Transmission of ITO/TiO_2/Au multilayers deposited on quartz SiO_2. Au was deposited with 100, 200 and 400 laser pulses.

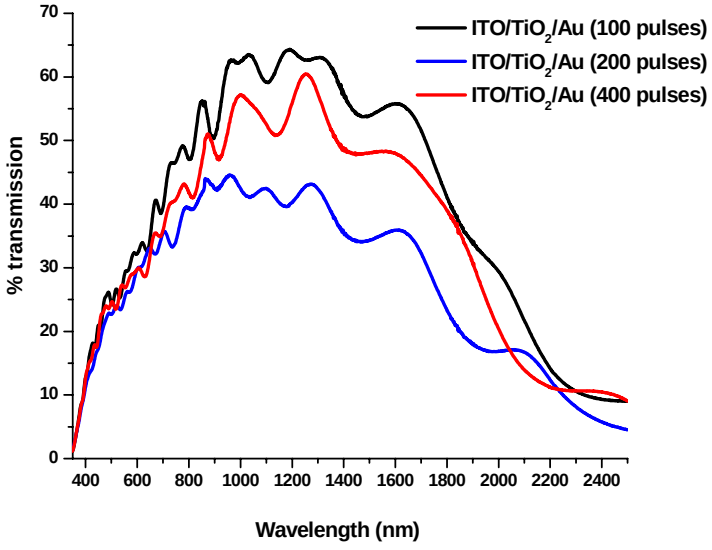

Figure 6.23 Transmission of ITO/TiO_2/Au multilayers deposited on quartz SiO_2. ITO/TiO_2 films were annealed at 500°C for 3 hours. Au was deposited with 100, 200 and 400 laser pulses at room temperature.

Fig.6.22 shows the transmittance of the different multilayers in the spectral range 300-2000nm. It can be seen from Fig.6.22 that the transmittance decreases from 92% to 70% in the Vis as the laser pulse number on the Au target increases from 100 to 400 pulses. Moreover, there is a sharp decrease of the transmission in the IR range with the increase of pulse number on the Au target: This suggests that the absorption of light is more intense in that range. This result proves that, upon addition of Au particles to TiO_2, the absorption of light intensity increases in a broader range which indicates that Au makes the ITO/TiO_2 bilayers sensitive not only to visible light but also to UV and IR. When the Au is deposited onto the ITO/TiO_2 annealed at 300°C and 500°C, the transmission decreases again steeply in the UV-Vis region, as shown in Fig.6.23.

6.2.4 Optical absorption and energy gap

As briefly mentioned in Chapter 3, both experimental results and theoretical calculations suggest that rutile TiO_2 has a direct forbidden gap (3.03eV), which is almost degenerated with an indirect allowed transition (3.05eV) [320, 321]. Due to the weak strength of the direct forbidden transition, the indirect allowed transition dominates in the optical absorption just above the absorption edge. In contrast, anatase and brookite TiO_2 are known as indirect band gap semiconductor. The fundamental absorption edge of anatase crystals was determined to be 3.2eV at room temperature and 3.3eV at 4K [322]. We are not aware of any reported experimental data for brookite.

However, since there are only minor differences in local crystal environment between anatase and brookite, the electronic structure and properties should be similar between the two phases. The calculated indirect band gap of brookite was 2.22eV [323] while the one of anatase crystal was found at 2.04eV, which is by far (~1.16eV) lower than the experimental value. In indirect band gap semiconductor, the absorption occurs in a different way as compared to that in a direct band gap semiconductor. In the case of an indirect band gap semiconductor, the minimum energy in the conduction band and the maximum energy in the valence band occur at different values of crystal momentum.

Photon energy, much larger that the forbidden gap, is required to give direct transitions from the valence to the conduction band. However, transitions can occur at lower energies by a two step process involving not only photons and electrons, but also a third particle, a phonon. A phonon is just a fundamental particle corresponding to the coordinated vibration of the atoms making up the crystal structure. As opposed to photons, phonons have a low energy but relatively a high momentum. An electron can make a transition from the maximum energy in the valence band to the minimum energy in the conduction band in the presence of photon of suitable energy by the emission or absorption of a phonon of the required momentum. Thus the probability of light being absorbed by this process is much less and gives rise to an absorption edge that is less steeped than in the direct band gap case. Hence, the absorption coefficient is low and light can pass a reasonable distance into the semiconductor prior to absorption.

For indirect allowed transition, the absorption coefficient, when scattering effects are neglected, can be calculated from the following formula [322]:

$$(\alpha h\nu)^{1/2} = \alpha_0 (h\nu - E_g) \tag{6.10}$$

where α is the absorption coefficient, α_0 is a constant having a numerical value $2x10^4$ when α is expressed in cm^{-1} and $h\nu$ and E_g in eV.

The optical band gap E_g of the single layer TiO_2 thin film was determined from Eq. (6.10). The band gap has been investigated by plotting $(\alpha h\nu)^2$ vs $h\nu$ (for direct allowed transitions) and $(\alpha h\nu)^{1/2}$ vs $h\nu$ (for indirect allowed transitions) for the different films. In the present study, the best straight line plot extended over most of data points. Fig.6.24 shows plots of $(\alpha h\nu)^{1/2}$ vs $h\nu$ (a) and $(\alpha h\nu)^2$ vs $h\nu$ (b) for TiO_2 deposited on quartz SiO_2 at 400°C and annealed at 500°C for 3 hours

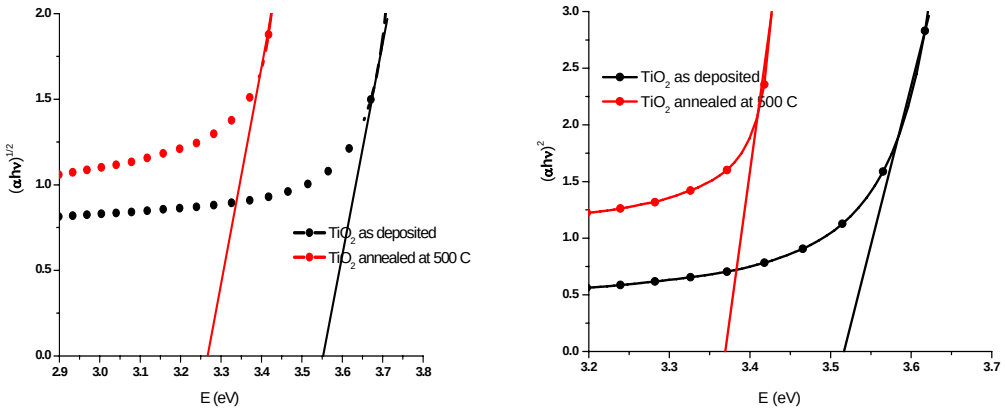

(a) (b)

Figure 6.24 Plots of $(\alpha h\nu)^{1/2}$ vs hν (a) and $(\alpha h\nu)^2$ vs hν for TiO_2 deposited on quartz SiO_2 at 400°C and annealed at 500°C for 3 hours.

These TiO_2 films present a direct band gap of 3.51eV and 3.37eV for the as deposited and annealed films, respectively. The indirect band gap is found to be 3.55eV and 3.26eV for TiO_2 films as deposited and after annealing, respectively. These results suggest that the TiO_2 films annealed at 500°C have the anatase structure (3.2eV) [245]. This agrees well with the XRD and Raman measurements (previous chapter).

It was already reported [248, 324, 325] a decrease in band gap as annealing of the film is performed. Such shift cannot be explained only in terms of phase transition of the film. One possibility is that the structure of TiO_2 films may be strongly affected by the strain effect from lattice distortion [248]. At high temperatures, particles have enough migration energy to rearrange after the adsorption. In such case, the shift might be caused by a change in the film optical density, i.e., the product of refractive index and thickness, which probably results from film densification and change in refractive index of mixed phases [325].

Fig.6.25 shows plots of $(\alpha h\nu)^2$ vs hν for ITO, ITO/TiO_2 and ITO/TiO_2/Au films. The ITO has been deposited at 200°C, TiO_2 films were deposited at 200°C (a) and 400°C (b). 500 laser pulses were used to deposit Au on top of TiO_2 layer at room

temperature. As can be seen in Fig.6.25, there is a shift of about 0.1eV between the ITO film deposited at 200°C and the ITO/TiO_2 layers deposited at 200°C. The shift (0.1eV) decreases by half when TiO_2 film is deposited at 400°C onto an ITO layer. Plots of $(\alpha h\nu)^{1/2}$ vs hν did not show a good enough linear region. This decrease of the band gap is in agreement with the transmittance data of both samples.

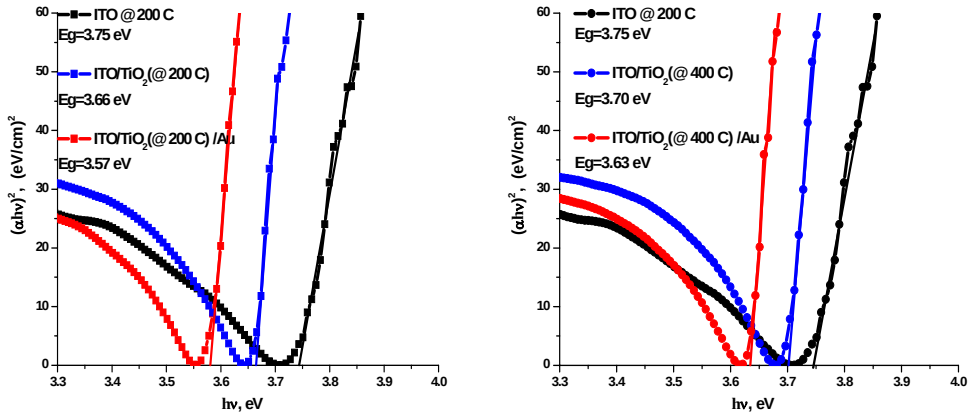

(a) (b)

Figure 6.25 Plots of $(\alpha h\nu)^2$ vs hν for ITO, ITO/TiO_2 and ITO/TiO_2/Au films. The ITO has been deposited at 200°C; TiO_2 was deposited at 200°C (a) and 400°C (b). Au was deposited on top of TiO_2 at room temperature using 500 laser pulses.

A low transmittance (thus a high absorption) for ITO/TiO_2 bilayers deposited at 200°C indicated that part of the photons impinging on the surface of TiO_2 film was absorbed, as compared with the ITO/TiO_2 films where the TiO_2 is deposited at 400°C, which shows higher transparency (low absorption). This is likely due to a higher concentration of crystalline defects that smear the band edges and introduce mid-gap states, thereby lowering the band gap of the material.

It is important to notice the shift towards shorter wavelengths from 3.56 to 3.63eV for the ITO/TiO_2/Au and ITO/TiO_2 multilayers, respectively, where TiO_2 is deposited at 200°C and from 3.66 to 3.70eV for ITO/TiO_2/Au and ITO/TiO_2

multilayers, respectively, where TiO_2 is deposited at 400°C. In this case, the increase of E_g can be attributed to a reduction of the oxygen vacancies with increasing substrate temperature at which ITO film has been previously deposited. In this regard, the quantum-size effect influenced the position of the absorption edge. The smaller the particle sizes, the higher the band-gap energy [304]. Fig.6.26 shows plots of $(\alpha h\nu)^2$ vs hν for ITO/TiO_2/Au multilayers. TiO_2 was deposited at 400°C and Au was deposited with 100, 200 and 400 laser pulses on top of TiO_2 film at room temperature. Fig.6.26 (a) refers to as deposited film, and (b) to a film annealed at 500°C for 3 hours. Interesting features are shown in these graphs. A high optical band gap is found for all the films

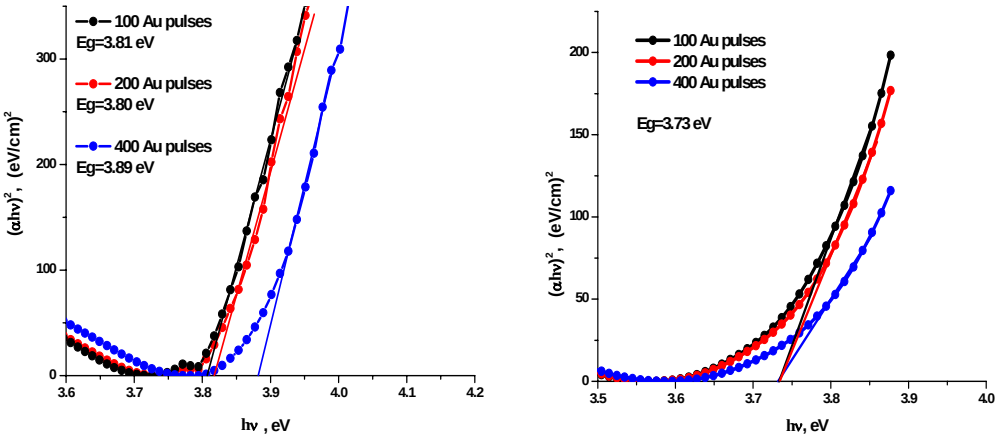

(a) (b)

Figure 6.26 Plots of $(\alpha h\nu)^2$ vs hν for ITO/TiO_2/Au multilayers. TiO_2 was deposited at 400°C and 100, 200 and 400 laser pulses were used to deposit Au on top of TiO_2 at room temperature. (a) as deposited and (b) after annealing at 500°C for 3 hours.

One can first note the shift toward smaller wavelength with increase of Au pulses for multilayer films deposited without annealing. The band gap is 3.80, 3.81 and 3.89eV, respectively, for 100, 200 and 400 laser pulses on the Au target. The shift is quite insignificant from 100 to 200 pulses, but it is more pronounced when the pulses are 400. In contrast, when the ITO/TiO_2 is annealed at 500°C before

depositing the Au nanoparticles, the gap energy is not affected and remains 3.73eV, close to that of the bilayer ITO/TiO_2 (deposited at 400°C). This suggests that the ITO/TiO_2 bilayer crystalline structure is not much affected by the gold deposition. The fact that E_g is the almost the same after Au deposition with 100, 200 or 400 pulses on ITO/TiO_2 means that the films may also have a common short-range order at a nanoscale. The details regarding the electronic state of the produced ITO/TiO_2 bilayers remain unclear. However, the change in the shape of the fundamental absorption edge is considered to reflect the variation of density and the short-range structural modifications undetected by the structural analysis.

In heavily doped semiconductor, the absorption edge lies at much shorter wavelength as compared to the intrinsic case. This is known as a Moss-Burstein shift. Interband optical transitions, which can be described by wave functions localised over distances of the order of the lattice constant, are relatively unchanged by disorder [325-328]. Therefore, optical E_g estimated from $(\alpha h\nu)^2$ vs $h\nu$ and $(\alpha h\nu)^{1/2}$ vs $h\nu$ reflects the electronic structure of the material, which in turn reflects its local atomic structure that may not be detected by structural characterisation. That is, these parameters can be correlated with the short-range order at the nanoscale and particularly with an amorphous phase, alone or coexisting with crystalline materials in films grown at low temperatures.

6.3 Conclusion

ITO films of different thicknesses have been produced by PLAD at different oxygen pressure and different temperature substrates. It was proved that the ITO films have a very high transmittance in the visible range. The transmittance, in the wavelength range above 800nm, decreased steeply by the plasma effect due to large carrier concentrations. All films produced at room temperature within the pressure range 1 to 10Pa were very transparent. The transmission of visible light is above 88% for films produced at room temperature and above 95% for the one deposited at 200°C, the transmission for the films produced in oxygen is about 90% above 400nm. Decreasing oxygen pressure leads to an increase of oxygen vacancies and thus increased conductivity of the films. However, this increase in

oxygen vacancies also leads to a decrease in the optical transmittance due to an increase in free carrier absorption.

The band gap and the refractive index for the ITO films were strongly affected by deposition conditions such as oxygen pressure. An increase in the band gap was observed by increasing the oxygen pressure. The change is due to an increase in carrier concentration in the films. A reduction of the refractive index for ITO films can be achieved by raising the electron density in the films, which can be obtained by increasing deposition temperature or increasing oxygen pressure. An increase of band gap has also been observed by increasing the temperature of substrate. This has been attributed to the Burstein-Moss shift also related to the carrier concentration.

On the other hand, optical properties of TiO_2 thin films deposited on heated and unheated quartz SiO_2, as well as the Si substrates, in oxygen atmosphere have been investigated. The transmission of the light intensity is lower in Si than in SiO_2. This is due to the fact the used Si wafers transmit only ~22% of the light in the near IR region. It has been found that increasing the SiO_2 substrate temperature from room temperature to 400°C resulted in an increase of the transmission mostly in the Vis-near IR from about 70 to 92%. After annealing at 500°C for 3 consecutive hours, the transmission of TiO_2 film sharply decreases toward shorter wavelengths. This behaviour is explained in terms of change in crystallinity of the TiO_2 thin film. It can also be explain in terms of the Burstein-Moss effect as the conduction band is pushed to higher energies by the increase in carrier concentration.

The refractive index measured at 550nm was 2.33 for the TiO_2 deposited at 400°C on Si and 2.04 for TiO_2 deposited in SiO_2. The refractive index of TiO_2 thin film deposited at 400°C on SiO_2 was found to increase with annealing temperature. This is in agreement with a decreasing band gap observed for the same films. Analysis of the transmittance curve of TiO_2/Au shows a decrease of about 6% of the transmission in the UV-Vis range. This decrease is due to the Au nanoparticles

deposited on top of the TiO_2 thin films. The Au particles might have absorbed a part of light, since their plasmon resonance lies around 520nm. The transmission of the ITO/TiO_2 bilayer, where the TiO_2 thin film is deposited at 400°C, is higher than that of the ITO/TiO_2 bilayer where the TiO_2 thin film is deposited at 200°C. When Au is further deposited on the above bilayer, the transmission decreased about 10% from it initial value.

The optical absorption edge analysis showed that the optical density could sensitively detect the film growth behavior, and correlate the film structure and the absorption edge. The TiO_2 films present a direct band gap at 3.51eV and 3.37eV for TiO_2 as deposited and after annealing, respectively, while the indirect band gap is found to be 3.55eV and 3.26eV for TiO_2 films as deposited and after annealing, respectively. There is a shift of about 0.1eV between ITO film deposited at 200°C and ITO/TiO_2 bilayers deposited at 200°C. The shift (0.1eV) decreases by half when the TiO_2 film is deposited at 400°C onto ITO layer. A shift towards shorter wavelengths from 3.56 to 3.63eV for ITO/TiO_2/Au and ITO/TiO_2 multilayers, respectively, where TiO_2 is deposited at 200°C, and from 3.66 to 3.70eV for ITO/TiO_2/Au and ITO/TiO_2 multilayers, respectively, where TiO_2 is deposited at 400°C, has been observed. In this case, the increase of E_g could be attributed to a reduction of the oxygen vacancies with increasing substrate temperature at which ITO film has been previously deposited.

The enlargement of band-gap energies of semiconductors is apparently a detrimental effect when these are employed as photo catalysts under visible irradiation, due to the significant decreasing of photon absorption by the semiconductors. Meanwhile, the increase of the band-gap energies of semiconductors used in DSSC may be advantageous to suppress the charge recombination between the reduced electrolytes and the photo-excited holes in the valence band of TiO_2 substrates and enhance the open-circuit potential of the cell. In addition, the enlargement of band gap semiconductor enhances their stability and corrosion resistance. When ITO/TiO_2 bilayers were annealed before depositing Au, the gap energy remained constant.

CHAPTER 7

GENERAL CONCLUSION AND PERSPECTIVES FOR FUTURE WORK

7.1 Theoretical investigations

In this work, the birth of pulsed laser ablation deposition has been investigated and the basic mechanism that rules the reactive ablation process has been extensively explained. It has been demonstrated that the use of a reactive gas pressure makes the method versatile. The possibility of additionally changing laser features, such as wavelength, repetition rate, pulse length, fluence and target-substrate distance, and the deposition conditions, such as substrate temperature and substrate orientation with respect to the deposited material, further demonstrates the enormous versatility of Pulsed Laser Ablation Deposition (PLAD).

Numerical, theoretical models and experimental techniques employed in the analysis of the laser-ablation process were reviewed. It has been explained that when nanosecond laser pulses are used, ablation occurs from both the melt and vapor phases and a considerable amount of material can be produced in a single shot. In this case, heat conduction into the solid target is the main source of energy loss. The combined Two Temperature Model-Molecular Dynamics (TTM-MD) model emerged as the most efficient tools for analysis of the short pulse laser interaction with metals. The method combines the advantages of TTM and MD for a realistic description of the diverse range of processes induced by short-pulse laser irradiation of a metal target. In addition, Monte Carlo simulations were proved to be the best method to handle laser plasma interaction. Monte Carlo can best handle this analysis. The model can be applied to any gas combination.

7.2 Experimental investigations

A coherent enhanced system for film growth by the PLAD and RPLAD has been described and improved. Large area approach makes use of the central part of the plume, which sweeps across the whole substrate. This situation was improved

when the target-substrate distance was increased, since the plume becomes wider when expanding away from the target. Uniform heating of the substrate was another challenge, because it is difficult to obtain a proper thermal contact over a large area. An alternative approach in designing a multi-substrate holder was investigated. The new system comprises three different substrate holders. The first one is a fixed holder accommodating one 60mm diameter flat substrate, which can be heated up to 800°C by a resistive heating system. The second substrate holder can translate independently along the x and y axes, to allow a uniform film deposition. It can accommodate a 100mm diameter flat substrate, which can be heated up to 400°C. The third substrate holder can accommodate three-dimensional substrates with a maximum length of 100mm and a maximum diameter of 50mm. It can translate and rotate simultaneously and can be heated up to 300°C by a lamp system.

7.3 Thin film deposition

In order to optimise film deposition conditions, a series of samples were deposited and many laser and chamber parameters were studied. Particularly, It was observed that:

- for the same pulse number, the thickness increase with the fluence. In this case, the ablation rate decreases slowly with increasing successive pulse number;
- the thickness uniformity was obtained; the thickness varies very little, the maximum variation in thickness was less than 10%;
- for the same pulse number, the thickness of the ITO film increases considerably with a decrease of laser wavelength. The effect was attributed to the photon energy in the laser pulse, since it is inversely proportional to the wavelength of the laser, which increase the absorption probability;
- the oxygen pressure was found to play a very important role on the film thickness, stoichiometry and resistivity.

One of the main features of this work was the achievement of a maximum deposition rates of 12nm/min for ITO and 21nm/min for TiO_2 thin film

deposition. These investigations allowed optimising the number of pulses used for the deposition and, therefore, to obtain a constant film thickness in the desired range. Best ITO and TiO_2 films were deposited under 1 and 10Pa of oxygen pressure with a thickness of 400 and 800nm, respectively. The best fluence was found to be 4J/cm^2 for both films, while it was 3J/cm^2 for the gold deposition. The oxygen pressure had a strong influence on the properties films deposited. In particular, films deposited in UHV without oxygen pressure were found to be thinner and non stoichiometric.

7.4 Structural and electrical properties

Another achievement of this work was the successful use of the RPLAD for ITO, TiO_2 and multilayers ITO/TiO_2 thin films, in UHV and O_2 atmospheres. Deposition was performed at room and high temperature on quartz SiO_2 (100) and silicon (111) substrates. Experimental conditions necessary to obtain crystalline layers with a high porosity and roughness were investigated. The deposited ITO films were highly orientated nanocrystals with their a-axis normal to the glass substrate surface. ITO films deposited at 200 and 400°C, were well crystallised with mean grains size of ~10nm and 15nm for ITO film deposited at 200 and 400°C, respectively. The onset of crystallisation resulted in the formation of a two layer structure containing a defective layer that decreased the carrier mobility.

Atomic Force Microscopy (AFM) studies revealed that the ITO thin films deposited were highly porous with a density of ~125holes/μm^2 samples deposited at 400°C. The porosity decreases with increasing the substrate temperature during deposition. The mean roughness was as high as 29.9nm, obtained in samples deposited at 400°C. Correlating the results between AFM and X-rays Diffraction (XRD), one can observe that for the ITO thin films deposited at 400°C, large grains correspond to well crystallised films with a preferential orientation along the (400) axis. This not withstanding, the ITO films remain very rough and porous at high temperatures. These morphological changes contributed to the improved optical and electrical properties through reduced scattering. The morphological properties observed for ITO films deposited at room temperature, 200 and 400°C

are shown to be well adapted for solar cell applications.

Low values of resistivity and high values of mobility were observed for the deposited ITO films. The resistivity of the film increases with increasing thickness, while it decreases when increasing the deposition temperature. It was found that the specific resistivity varies strongly

- with the oxygen pressure for the ITO films deposited at room temperature with a minimum value around $3x10^{-6}$ Ωm, corresponding to pressure of 1Pa;
- with the substrate temperatures; at 200°C the resistivity is lower with values around $1.5x10^{-6}$Ωm for a film thickness of 400nm.

The achievement of the lowest possible resistivity is of practical significance because it provides some freedom in selecting the film thickness to achieve a high optical transmission, while still maintaining low resistivity. In fact, as the substrate temperature increases, there is formation of crystalline grains which reach a diameter of about 10nm at 400°C, thus reducing collisions of the charge carrier with the grain boundaries. Hall mobility was found to increase with substrate temperature. In this investigation, the highest Hall mobility at room temperature was estimated to be $22.3cm^2/Vs$ under PO_2 of 1Pa and 52.1 and $51.3cm^2/Vs$ for films deposited at 200 and 400°C, respectively.

TiO_2 films, with a high specific surface area due to porosity, were annealed at 300 and 500°C for 3 consecutive hours. Raman spectra showed that annealing produced formation of pure anatase TiO_2 films, both on quartz SiO_2 glass substrate and on ITO predeposited films. Scanning Transmission Electron Microscopy (STEM) measurements suggested that TiO_2 films deposited at room temperature are rougher than the films deposited at 200 and 400°C. Moreover, TiO_2 film deposited on the predeposited ITO film present a porous surface, with an average pore diameter of ~ 40nm, and excellent uniformity. It is interesting to note that the pores are randomly arranged, in contrast to the ordered structures reported for dip-coated films. The random arrangement of the pore network may

actually be beneficial for producing uniform electrodes. The cross-sectional analysis of the films showed a columnar structure, but no evidence of voids in the structure.

The present results indicate that highly orientated nanocrystalline ITO films can be prepared on a SiO_2 glass substrate without post annealing treatments. Rutherford backscattering spectrometry investigations showed that ITO films free of any kind of contamination were deposited. The obtained films were uniform and highly stoichiometric over a large area. Porous oxides represent an interesting material for Dye Sensitised Solar Cells (DSSC). Nanoporous titania with a large surface area is usually required to support a large amount of dye for obtaining a high energy conversion efficiency. If the electrode used in a dye-sensitised solar cell is nano-porous, the pores are expected not only to provide a huge surface area, which can support a larger amount of functional materials of titania and dye, but also to decrease the thickness of titania layer. Consequently, the large surface area formed by the porous electrodes may increase photoelectric device's functions such as the energy conversion efficiency drastically. Moreover, the specific surface area of TiO_2 is closely related with its particle size. The smaller the particle sizes in TiO_2 films, the larger the specific surface area thereof.

7.5 Optical properties

The transmission of ITO films in visible light was above 88% for films produced at room temperature and above 95% for the ones deposited at 200°C. in addition, the transmission for the films produced in oxygen was about 90% above 400nm, whereas the value lies between 70 and 80% for films produced in rare gases. The bandgap and the refractive index for the ITO films were strongly affected by deposition conditions such as oxygen pressure. An increase in the bandgap was observed with increasing the oxygen pressure. This change is due to an increase in carrier concentration in the films. An increase of band gap has also been observed with increasing the temperature of substrate. This has been attributed to the Burstein-Moss shift which is also related to carrier concentration.

On the other hand, optical properties of TiO_2 thin films deposited on heated and unheated quartz SiO_2, as well as the Si substrates, in O_2 atmosphere have been investigated. The transmission of the light intensity is lower in Si than in SiO_2. This was due to the fact that the Si wafers used transmit only ~22% of the light in the near IR region. Increasing the SiO_2 substrate temperature from room temperature to 400°C resulted in an increase of the transmission mostly in the Vis-near IR, from about 70% to 92%. After annealing at 500°C for 3 consecutive hours, the transmission of TiO_2 films further sharply decrease toward shorter wavelengths. This behavior has been explained in terms of change in crystallinity of the TiO_2 thin film.

The refractive index measured at 550nm was 2.33 for the TiO_2 deposited at 400°C on Si and 2.04 for TiO_2 deposited on SiO_2. The refractive index of TiO_2 thin film deposited at 400°C on quartz SiO_2 was found to increase with annealing temperature. This is in agreement with a decreasing band gap observed for the same films. Analysis of the transmittance curve forTiO_2/Au shows a decrease of about 6% of the transmission in the UV-Vis range. This decrease was attributed to the Au nanoparticles deposited on top of the TiO_2 thin films. The Au particles might have absorbed part of light, since their plasmon resonance lies in the visible region. The transmission of the ITO/TiO_2 bilayer, where the TiO_2 thin film is deposited at 400°C, is higher than that of the ITO/TiO_2 bilayer where the TiO_2 thin film is deposited at 200°C. When Au is further deposited on the ITO/TiO_2 bilayer, the transmission decreased about 10% from its initial value.

The optical absorption edge analysis showed that the optical density could serve to sensitively detect the film growth behavior, and to correlate the film structure and the absorption edge. The TiO_2 films obtained present a direct band gap of 3.51eV and 3.37eV for TiO_2 as deposited and after annealing, respectively, while the indirect band gap is found to be 3.55eV and 3.26eV for TiO_2 films as deposited and after annealing, respectively. There was a shift in the direct band gap of about 0.1eV between ITO film deposited at 200°C and ITO/TiO_2 bilayers deposited at 200°C. A shift towards shorter wavelengths from 3.56 to 3.63eV for

ITO/TiO_2/Au and ITO/TiO_2 multilayers, respectively, where TiO_2 is deposited at 200°C, and from 3.66 to 3.70eV for ITO/TiO_2/Au and ITO/TiO_2 multilayers, respectively, where TiO_2 is deposited at 400°C, has been observed. In this case, the increase of E_g was ascribed to a reduction of the oxygen vacancies with increasing substrate temperature at which the ITO film had been previously deposited.

The change in the shape of the fundamental absorption edge is considered to reflect the short-range structural modifications undetected by structural characterisations. The enlargement of band-gap energies of semiconductors, which to some extent may be a detrimental effect when these are employed as photocatalysts under visible irradiation, may be advantageous when used in DSSC to suppress the charge recombination between the reduced electrolytes and the photo-excited holes in the valence band of TiO_2 substrates and enhance the open-circuit potential of the cell. However, when ITO/TiO_2 bilayers were annealed before depositing Au nanoparticles, the gap energy remained constant.

7.6 Perspectives for future work

The films prepared were extremely well adherent, quite hard, and show good electrical and optical properties. The present work demonstrated the feasibility of preparing multilayer ITO/TiO_2/Au by the RPLAD method in a single deposition. The incorporation of Au particles on the ITO/TiO_2 films under selected conditions was found to shift the energy gap of the multilayer. In order for this method to be more widely utilised, further work must be done, primarily in the areas of apparatus optimisation and sample characterisation. If completed, both areas would yield a wealth of information about the process itself, and how to prepare multilayer films with specific properties in view of industrial applications.

The possible applications in DSSC of films deposited in this investigation were extensively demonstrated throughout thesis. However, it is of great interest that DSSC can be built based on the films deposited and the spectral response be measured to evaluate the energy efficiency.

REFERENCES

[1] A. Einstein "*Zur Quantentheorie der Strahlung*", Physika Zeitschrift, 18, 121, 1917. Translated as "*Quantum Theory of Radiation and Atomic Processes*" H. A. Boorse and L. Motz (eds.). The World of the Atom **2**, (1966) 884.

[2] T. H. Maiman, "*Stimulated optical radiation in ruby*", Nature **187**, (1960) 493.

[3] J.C. Miller ed. "*Laser Ablation Principles and Applications*", Springer-Verlag, Berlin 1994.

[4] R. D. Schaeffer "*A closer look at laser ablation*", Laser Focus World **37**, (2001) 217.

[5] F. Breech and L. Cross, "*Optical microemission stimulated by a ruby maser*" Appl. Spectrosc **16**, (1962) 59.

[6] H.M. Smith and A.F. Turner, "*Vacuum deposited thin films using a Ruby laser*", Appl. Opt. **4** (1965) 147.

[7] S. Pellicori, "*Choosing Between Thermal Evaporation and Sputter Deposition*", Coating Material News **10** (2000).

[8] P. K. Caroll, E T Kennedy, G. O Sullivan, "*Laser-produced continua for absorption spectroscopy in the VUV and XUV*", Appl. Opt. **19** (1980) 1454.

[9] C. Veillet, J.F Mangin, J.E Chabaudie, C. Dumoulin, D. Feraudy, J.M Torre, "*Lunar laser ranging at CERGA for the ruby period (1981-1986), in Contributions of Space Geodesy to Geodynamics: Technology*", AGU Geodynamics Series **25**, edited by D.E Smith and D.L Turcotte, (1993) 133.

[10] D. Dijkkamp, T. Venkatesan, XD. Wu, S.A. Shaheen, N. Jisrawi, Y.H. Min-Lee, W.L. McLean, and M. Croft, "*Preparation of Y-Ba-Cu oxide superconductor thin films using pulsed laser evaporation from high-Tc bulk material*", Appl. Phys. Lett. **51** (1987) 619.

[11] E. Fogarassy, C. Fuchs, A. Slaoui, and J. P. Stoquert, "*SiO_2 thin-film deposition by excimer laser ablation from SiO target in oxygen atmosphere*" Appl. Phys. Lett.**57** (1990) 664.

[12] I.N. Mihailescu, N. Chitica, L.C. Nistor, M. Popescu, V.S. Teodorescu, I. Ursu, A. Andrei, A. Barborica, A.Luches, M.L. De Giorgi, A. Perrone, B.

Dubreuil, and J. Hermann, "*Deposition of high quality TiN films by excimer laser ablation in reactive gas*", J. Appl. Phys. **74** (1993) 5781.

[13] H. U. Krebs and O. Bremert, "*Pulsed laser deposition of thin metallic alloys*", Appl. Phys. Lett. **62** (1993) 2341.

[14] D.B. Chrisey and G.K. Hubler, eds., "*Pulsed Laser Deposition of Thin Films*", John Wiley & Sons, New York (1994).

[15] J. T. Cheung, I.M. Gergis, J. James and R. E. DeWames, "*Reproducible growth of high quality $YBa_2Cu_3O_{7-x}$ film on (100) MgO with a $SrTiO_3$ buffer layer by pulsed laser deposition*", Appl. Phys. Lett. **60** (1992) 3180.

[16] J. A. Greer, "*Commercial Scale-Up of Pulsed Laser Deposition*" in Pulsed Laser Deposition of Thin Films, D. B. Chrisey and G. K. Hubler (editors), John Wiley & Sons Inc., New York, 1994.

[17] Wiesendanger, "*Scanning Probe Microscopy and Spectroscopy Methods and Applications*". Cambridge, 1994.

[18] D. Chescoe and P. J. Goodhew, "*Operation of Transmission and Scanning Electron Microscopes*", Oxford, 1990.

[19] W.K. Chu, J.W. Mayer, and M.A. Nicolet, "*Backscattering Spectrometry*", Academic Press, New York, 1978.

[20] J. I. Goldstein, D. E. Newbury, P. Echlin, D. C. Joy, C. Fiori, E. Lifshin, "*Scanning Electron Microscopy and X-Ray Microanalysis: A Text for Biologists, Materials Scientists, and Geologists*", Plenum Press, 1984.

[21] S. L. Flegler, J. W. Heckman, Jr. K. L. Klomparens, "*Scanning and Transmission Electron Microscopy: An Introduction*", Oxford, 1993.

[22] G. Herzberg, "*Infrared and Raman Spectra of Polyatomic Molecules*", Van Nostrand Reinhold, New York, 1945.

[23] L.E. Brus, "*Electron-electron and electron-hole interactions in small semiconductor crystallites: The size dependence of the lowest excited electronic state*", J Chem Phys **80** (1984) 4403.

[24] A. Mayer, M. Antonietti: "*Investigation of polymer-protected noble metal nanoparticles by transmission electron microscopy - control of particle morphology and shape*", Colloid & Polymer Science **276** (1998) 769.

[25] M. Haruta, "*Size- and support-dependency in the catalysis of gold*", catalysis today **36** (1997) 153.

[26] H. Scott, S. F. Brewer, "*Calculation of the electronic and optical properties of indium tin oxide by density functional theory*", Chemical Physics **300** (2004) 285.

[27] K. Y. Kima, S. B. Park, "*Preparation and property control of nano-sized indium tin oxide particle*", Materials Chemistry and Physics **86** (2004) 210.

[28] A. Ambrosini, A. Duarte, K. R. Poeppelmeier, M. Lane Carl R. Kannewurf, T. O. Mason, "*Electrical, Optical, and Structural Properties of Tin-Doped In_2O_3–M_2O_3 Solid Solutions (M=Y, Sc)*", J. Sol State Chem 153 (2000) 41.

[29] E. Fogarassy, C. Fuchs, A. Slaoui, S. de Unamuno, J.P. Stoquert, W. Marine, B. Lang, "*Low-temperature synthesis of silicon oxide, oxynitride, and nitride films by pulsed excimer laser ablation*", J. Appl. Phys. **76** (1994) 2612.

[30] S. Acquaviva, M.L. De Giorgi, L. Elia, M. Fernandez, G. Leggieri, A. Luches, M. Martino, A. Zocco, "*Laser deposition of thin SiO_2 and ITO films*", Appl. Surf. Sci. **168** (2000) 244.

[31] G. Benko, B. Skarman, R. Wallenberg, A. Hagfeldt, V. Sundstrom, A. P. Yartsev, "*Particle Size and Crystallinity Dependent Electron Injection in Fluorescein 27-Sensitised TiO_2 Films*", J. Phys. Chem. B **107** (2003) 1370.

[32] T.M.R. Viseu, B. Almeida, M. Stchakovsky, B. Drevillon, M.I.C. Ferreira, J.B. Sousa, "*Optical characterisation of anatase: a comparative study of the bulk crystal and the polycrystalline thin film*", Thin Solid Films **401** (2001) 216.

[33] R. Ktinenkamp, R. Henninger, and P. Hoyer, "*Photocarrier transport in colloidal titanium dioxide films*", J. Phys. Chem **97** (1993) 7328.

[34] S. Yamamoto, T. Sumita, Sugiharuto, A. Miyashita, H. Naramoto, "*Preparation of epitaxial TiO_2 films by pulsed laser deposition technique*", Thin Solid Films **401** (2001) 88.

[35] J.M lackner, W Waldhauser, W. R. Ebner, B. Major, T. Schoberle, "*Pulsed laser deposition of titanium oxide coatings at room temperature-*

structural, mechanical and tribological properties" Surface and Coatings Technology **585** (2004) 180.

[36] T. G. Lei, H. H. Bo, S. J. Da, "*Effect of Microstructure of TiO_2 Thin Films on Optical Band Gap Energy*", Chinese physics letters, **22** (2005) 1787.

[37] K. Maki, N. Komiya, A. Suzuki, "*Fabrication of thin films of ITO by aerosol CVD*", Thin Solid Films **445** (2003) 224.

[38] E. Benamar, M. Rami, C. Messaoudi, D. Sayah, A. Ennaoui, "*Structural, optical and electrical properties of indium tin oxide thin films prepared by spray pyrolysis*", Solar Energy Mater and Solar Cells **56** (1998) 125.

[39] M. Yamaguchi, A. Ide-Ektessabi , H. Nomura , N. Yasui, "*Characteristics of indium tin oxide thin films prepared using electron beam evaporation*", Thin Solid Films **447** (2004) 115.

[40] T.C. Gorjanc, D. Leong, C. Py, D. Roth, "*Room temperature deposition of ITO using r.f. magnetron sputtering*", Thin Solid Films **181** (2002) 413.

[41] M. Martino, A. Luches, M. Fernandez, P. Anobile, V. Petruzzelli, "*Characterisation of thin indium tin oxide films deposited by pulsed XeCl laser ablation*", J. Phys. D: Appl. Phys. **34** (2001) 2606.

[42] A.P. Caricato, M. De Sario, M. Fernandez, G. Leggieri, A. Luches, M. Martino, F. Prudenzano, "*Pulsed laser deposition of materials for optoelectronic applications*", Appl. Surf. Sci. **197-198 (**2002) 458.

[43] J. B. Choi, J. H. Kim, K. Ah-Jeon, S. Y. Lee, "*Properties of ITO films on glass fabricated by pulsed laser deposition*", Mater. Sci. and Engineer **B102** (2003) 376.

[44] B. Thestrup, J. Schou, A. Nordskov, N. B. Larsen, "*Electrical and optical properties of thin indium tin oxide films produced by pulsed laser ablation in oxygen or rare gas atmospheres*", Appl. Surf. Sci. **142** (1999) 248.

[45] R.K. Singh, D. Kumar, "*Pulsed laser deposition and characterisation of high-T_c $YBa_2Cu_3O_{7-x}$ superconducting thin films*", Material Science and Engineering **R22 (**1998) 113.

[46] D. S Chuu, Yu-Ching Chang and Cheng-Ying Hsieh, "*Growth of CdMnS films by pulsed laser evaporation*", Thin Solid Films **304** (1997) 28.

[47] O. Masayuki, H. Kouji, H. Mitsugu, "*Pulsed laser deposition of ZnO thin films using a femtosecond laser*", Appl. Surf. Sci. **154-155 (**2000) 424.

[48] R.E H. Sims, "*Renewable energy: a response to climate change*", Solar Energy **76** (2004) 9.

[49] S.H. Kim, C. M. Cracken, J. Edmonds, "*Solar energy technologies and stabilising atmospheric CO_2 concentrations*", Prog. Photovolt. Res. Appl. **8 (**2000) 3.

[50] M. Grätzel, "*Photoelectrochemical cells*", Nature **414** (2001) 328.

[51] B. O'Regan, M. Grätzel, "*A low-cost, high efficiency solar cell based on dye-sensitised colloidal TiO_2 films*", Nature **353** (1991) 737.

[52] L. Kavan, M. Grätzel, S. E. Gilbert, C. Klemenz, H. J. Scheel, "*Electrochemical and photoelectrochemical investigations of single-crystal anatase*". J. Am. Chem. Soc. **118** (1996) 6716.

[53] M. Grätzel, "*Low-cost solar cells*", The World & I, (1993) 228.

[54] A. Hagfeldt, & M. Grätzel, "*Molecular photovoltaics*". Acc. Chem. Res. **33** (2000) 269.

[55] G. Phani, G. Tulloch, D. Vittorio, I. Skryabin, "*Titania solar cells: new photovoltaic technology*", Renewalable Energy **22** (2001) 303.

[56] A. Fujishima. K. Honda, "*Electrochemical photolysis of water at a semiconductor electrode*", Nature **238**, (1972) 37.

[57] J. Krüger, U. Bach, M. Grätzel, "*High efficiency solid-state photovoltaic device due to inhibition of interface charge recombination*", Appl. Phys. Lett. **79**, (2001) 2085.

[58] E. Stathatos, P. Lianos, U. L. Stangar, B. Orel, "*A high-performance solid-state dye-sensitised photoelectrochemical cell employing a nanocomposite gel electrolyte made by the sol-gel route*", Adv. Mater. **14** (2002) 354.

[59] W. Kubo, S. Kambe, S. Nakade, T. Kitamura, K. Hanabusa, Y. Wada, S. Yanagida, "*Photocurrent-Determining Processes in Quasi-Solid-State Dye-Sensitised Solar Cells Using Ionic Gel Electrolytes*" J. Phys. Chem. **B 107** (2003) 4374.

[60] E. W. Macfarland, J. Tang, "*A photovoltaic device structure based on internal electron emission*", Letter to nature **421** (2003) 616.

[61] M. Seah, W. A Pand Dench, "*Quantitative electron spectroscopy of surfaces: A standard data base for electron inelastic mean free paths in solids*", Surface Interface Anal. **1** (1979) 2.

[62] K. W. Frese, C. Chen, "*Theoretical models of hot carrier effects at metal-.semiconductor electrodes*", J. electrochem. Soc. **139** (1992) 3234.

[63] C. Wen, K. Ishikawa, M. Kishima, K. yamada, "*Effects of silver particles on the photovoltaic properties of dye-sensitised TiO_2 thin films*", Solar Energy mater. and Solar. cells **61**, (2000) 339.

[64] F. Fotsa Ngaffo, S. Ekambaram, O. Nemraoui, M. Witcomb, M. Maaza, "*Synthesis of Hybrid nanomaterials PMMA-Au by laser/spin coating and laser/lyophilisation*" Proc. of the 2nd Intenational Conferences of the Africa MRS, University of the Witwatersrand, Johannesburg, South Africa (2003) 247.

[65] C. Belouet, "*Thin film growth by the pulsed laser assisted deposition technique*", Appl. Surf. Sci. **96-98** (1996) 630.

[66] R. Teghil, V. Marotta, A. G. Guidoni, T.M. Di Palma, C. Flamini, "*Reactive pulsed laser ablation and deposition of thin indium tin oxide films for solid state compact sensors*", Appl. Surf. Sci. **138-139 (**1999) 522.

[67] I.N. Mihailescu, N. Chitica, V.S. Teodorescu, M.L. De Giorgi, G. Leggieri, A. Luches, M. Martino, A. Perrone, B. Dubreuil, "*Excimer laser reactive ablation: an efficient approach for the deposition of high quality TiN films*", J. Vac. Sci. Technol. **A 11** (1993) 2577.

[68] A. Luches, E. D'Anna, G. Leggieri, S. Luby, E. Majovka, G. Majni, P. Mengucci, "*Iron silicide formation by excimer laser pulses*", SPIE Proc. **205** (1994) 2045.

[69] I.N. Mihailescu, N. Chitica, V.S. Teodorescu, M. Popescu, M.L. De Giorgi, A.Luches, A. Perrone, Ch. Boulmer-Leborgne, J. Hermann, B. Dubreuil, A. Barborica, I. Iova, "*Direct carbide synthesis by multipulse excimer laser treatment of Ti samples in ambient CH_4 gas at superatmospheric pressure*", J. Appl. Phys. **75** (1994) 5286.

[70] A. Luches, G. Leggieri, M. Martino, A. Perrone,G. Majni, P. Mengucci, and, I.N. Mihailescu, "*Laser reactive ablation deposition of nitride films*", Appl. Surf. Sci. **79-80** (1994) 244.

[71] S. Fahler, M. Störmer, and H. U. Krebs, "*Origin and avoidance of droplets during laser ablation of metals*", Appl. Surf. Sci. **109-110** (1997) 433.

[72] R. Kelly, and J. E. Rothenberg, "*Laser sputtering: Part III. The mechanism of the sputtering of metals low energy densities*", Nucl. Instrum. Methods Phys. Res. **B 7-8**, (1985) 755.

[73] R. K. Singh and J. Narayan, "*Pulsed-laser evaporation technique for deposition of thin films: Physics and theoretical model*", Phys. Rev. **B 41** (1990) 8843.

[74] B. Holzapfel, B. Roas, L. Schultz, P. Bauer, and G. S. Ischenko, "*Off-axis laser deposition of $YBa_2Cu_3O_{7-\delta}$ thin films*", Appl. Phys. Lett. **61**, (1992) 3178.

[75] A. A. Gorbunov, W. Pompe, A Sewing, S. V. Gaponov, A. D. Akhsakhalyan, I. G. Zabrodin, I. A. Kaskov, E. B. Klyenkov, A. P. Morozov, N. N. Salaschenko, R. Dietsch, H.Mai, and S. Völlmar, "*Ultrathin film deposition by pulsed laser ablation using crossed beams*", Appl. Surf. Sci. **96-98** (1996) 649.

[76] N. Inoue, H. Yuasa, M. Okoshi, "*TiO_2 thin films prepared by PLD for photocatalytic applications*", Applied surface science **197-198** (2002) 393.

[77] S. Yamamoto, T. Sumita, T. Yamaki, A. Miyashita, H. Naramoto, "*Characterisation of epitaxial TiO_2 films prepared by pulsed laser deposition*", Journal of Crystal Growth **237-239** (2002) 569.

[78] F.Fotsa Ngaffo, A. P. Caricato , A. Fazzi, M. Fernandez, S. Lattante, M. Martino, F. Romano, "*Deposition of ITO films on SiO_2 substrates*", Appl. Surf. Sci. **248** (2005) 428.

[79] M. Balooch, R. J. Tench, W. J. Siekhaus, M. J. Allen, A. L. Connor, and D. R. Olander, "*Deposition of SiC films by pulsed excimer laser ablation*", Appl. Phys. Lett. **57 (**1990) 1540.

[80] C. M. Foster, K. F. Voss, T. W. Hagler, D. Mihailovic, A. J. Heeger, M. M.Eddy, W. L. Olsen, and E. J. Smith, "*Infrared reflection of epitaxial $Tl_2Ba_2CaCu_2O_8$ thin films in the normal and superconducting states*", Solid State Comm. **76** (1990) 651.

[81] J.C.S. Kools, T. S. Baller, S T De Zwart and J Dielemann, "*Gas flow dynamics in laser ablation deposition*", J. Appl. Phys. **71** (1992) 4547.

[82] D. Bäuerle, "*Laser processing and chemistry*", 3rd edition, Springer-Verlag (Berlin, 2000) 469.

[83] T. D. Bennett, C. P. Grigoropoulos, and D. J. Krajnovich, "*Near-Threshold Laser Sputtering of Gold*", J. Appl. Phys. **77** (1995) 849.

[84] L. V. Zhigilei, D. S. Ivanov, E. Leveugle, B. Sadigh, and E. M. Bringa, "*Computer Modeling of Laser Melting and Spallation of Metal Targets*", High Power Laser Ablation V, Proc. SPIE **5448** (2004) 505.

[85] S. I. Anisimov, B. L. Kapeliovich, and T. L. Perel'man, "*Electron Emission from Metal Surfaces Exposed to Ultrashort Laser Pulses*", Zh. Eksp. Teor. Fiz. **66** (1974) 776. [Sov. Phys. JETP 39, 375 (1974)].

[86] B. Rethfeld, A. Kaiser, M. Vicanek, G. Simon, "*Ultrafast Dynamics of Nonequilibrium Electrons in Metals Under Femtosecond Laser Irradiation*", Phys. Rev. **B 65** (2002) 214303.

[87] N.M. Bulgakova, R. Stoian, A. Rosenfeld, I. V. Hertel, E.E.B. Campbell, "*Electronic Transport and Consequences for Material Removal in Ultrafast Pulsed Laser Ablation of Materials*", Phys. Rev. **B 69** (2004) 054102.

[88] J. Hohlfeld, S.S. Wellershoff, J. Gudde, U. Conrad, V. Jahnke, and E. Matthias, "*Electron and Lattice Dynamics Following Optical Excitation of Metals*", Chem. Phys. **251** (2000) 237.

[89] S. S. Wellershoff, J. Hohlfeld, J. Gudde, E. Matthias, "*The Role of Electron- Phonon Coupling in Femtosecond Laser Damage of Metals*", Appl. Phys. **A 69** (1999) S99.

[90] P. J. Antaki, "*Importance of Nonequilibrium Thermal Conductivity During Short-Pulse Laser-Induced Desorption From Metals*", Int. J. Heat Mass Transfer **45** (2002) 4063.

[91] V. Schmidt, W. Husinsky, and G. Betz, "*Dynamics of Laser Desorption and Ablation of Metals at the Threshold on the Femtosecond Time Scale*", Phys. Rev.Lett. **85** (2000) 3516.

[92] T. Q. Qiu and C. L. Tien, "*Size Effects on Nonequilibrium Laser Heating of Metal Films*", J. Heat Transfer **115** (1993) 842.

[93] J. K. Chen, J. E. Beraun, L. E. Grimes, and D. Y. Tzou, "*Modeling of Femtosecond Laser-Induced Nonequilibrium Deformation in Metal Films*", Int. J.Solids Struct. **39** (2002) 3199.

[94] L. A. Falkovsky and E. G. Mishchenko, "*Electron-Lattice Kinetics of Metals Heated by Ultrashort Pulses*", Zh. Eksp. Teor. Fiz. **115** (1999) 149.

[95] J. Hohlfeld, J. G. Müller, S.-S. Wellershoff, and E. Matthias, "*Time-Resolved Thermoreflectivity of Thin Gold Films and its Dependence on Film Thickness*", Appl. Phys. **A 64** (1997) 387.

[96] Z. H. Jin, P. Gumbsch, K. Lu, and E. Ma, "*Melting Mechanism at the Limit of Superheating*", Phys. Rev. Lett. **87** (2001) 055703-1.

[97] Z. H. Jin and K. Lu, "*Melting of Surface-Free Bulk Single Crystals*", Philos. Mag.Lett. **78** (1998) 29.

[98] L. V. Zhigilei and B. J. Garrison, "*Pressure Waves in Microscopic Simulations of Laser Ablation*", Mater. Res. Soc. Symp. Proc. **538** (1999) 491.

[99] L. V. Zhigilei and B. J. Garrison, "*Microscopic Mechanisms of Laser Ablation of Organic Solids in the Thermal and Stress Confinement Irradiation Regimes*", J. Appl. Phys. **88** (2000) 1281.

[100] L. V. Zhigilei, "*Dynamics of the Plume Formation and Parameters of the Ejected Clusters in Short-Pulse Laser Ablation*", Appl. Phys. A: Mater. Sci. Process. **76** (2003) 339.

[101] D. S. Ivanov and L. V. Zhigilei, "*Combined Atomistic-Continuum Model for Simulation of Laser Interaction with Metals: Application to Calculation of Melting Threshold in Ni Targets of Varying Thickness*", Appl. Phys. **A 79**, (2004) 977.

[102] Bauerle D, "*Laser Processing and Chemistry*", Berlin: Springer(ed) 1996.

[103] Bauerle D,"*Laser Processing and Diagnostics*", Berlin: Springer(ed) 1984.

[104] R. K. Singh and J. Narayan, "*A novel method for simulating laser-solid interactions in semiconductors and layered structures*", Mat. Sci. Engng **B 3** (1989) 217.

[105] A. Peterlongo, A. Miotello, R. Kelly, "*Laser-pulse sputtering of aluminum: Vaporisation, boiling, superheating, and gas-dynamic effects*", Phys. Rev. **E 50** (1994) 4716.

[106] A. Miotello, R. Kelly, "*Critical assessment of thermal models for laser sputtering at high fluences*", Appl. Phys. Lett. **67** (1995) 3535.

[107] N. Arnold, B. Lukyanchuk, N. Bityurin, "*A fast quantitative modelling of ns laser ablation based on non-stationary averaging technique*", Appl. Surf. Sci. **127–129** (1998) 184.

[108] B.C. Stuart, M. D. Feit, A. M Rubenchick, B. W. Shore, M. D. Perry, "*Laser-Induced Damage in Dielectrics with Nanosecond to Subpicosecond Pulses*", Phys. Rev. Lett. **74** (1995) 2248.

[109] J. Ihlemann, A. Scholl, H. Schmidt, B. W. Rottke, "*Nanosecond and femtosecond excimer-laser ablation of oxide ceramics*", Appl. Phys. **A 60** (1995) 411.

[110] N. B. Chichcov, C. Momma, S. Nolte, F. Von Alvensleben, A. Tünnermann, "*Femtosecond, picosecond and nanosecond laser ablation of solids*", Appl. Phys. **A 63** (1996) 109.

[111] R. Kelly and A. Miotello, "*Comments on explosive mechanisms of laser sputtering*", Appl. Surf. Sci. **96–98** (1996) 205.

[112] R. M. Gilgenbach and P.L.G. Ventzeck, "*Dynamics of excimer laser-ablated aluminum neutral atom plume measured by dye laser resonance absorption photography*", Appl. Phys. Lett. **58** (1991) 1597.

[113] S. Amoruso, V. Berardi, R. Bruzzese, N. Spinelli and X. Wang, "*Kinetic energy distribution of ions in the laser ablation of copper targets*", Appl. Surf. Sci. **127-129** (1998) 953.

[114] R. Timm, P. R. Willmott and J. R. Huber, "*Ablation and blow-off characteristics at 248nm of Al, Sn and Ti targets used for thin film pulsed laser deposition*", J. Appl. Phys. **80** (1996) 1794.

[115] R. K. Singh and J. Viatella, "*Estimation of plasma absorption effects during pulsed laser ablation of high-critical-temperature superconductors*", J. Appl. Phys. **75** (1994) 1204.

[116] X. Mao, R.E. Russo, "*Observation of plasma shielding by measuring transmitted and reflected laser pulse temporal profiles*" Appl. Phys **A. 64** (1996) 1.

[117] D.I. Rosen, J. Mitteldorf, G. Kothandaraman, A. N. Pirri and E. R. Pugh, "*Coupling of pulsed 0.35-μm laser radiation to aluminum alloys*", J. Appl. Phys. **53** (1982) 3190.

[118] C. R. Phypps, T. P. Turner, R F Harrison, G. W. York, W. Z. Osborne, G. K. Anderson, X. F. Corlis, L. C. Hayes, H. S. Steele and T. R. King, "*Impulse coupling to targets in vacuum by KrF, HF, and CO_2 single-pulse lasers*", J. Appl. Phys. **64**, (1988) 1083.

[119] S. Amoruso, R. Bruzzese, N. Spinelli, R. Velotta, "*Characterisation of laser-ablation plasmas*", J. Phys. B: At. Mol. Opt. Phys. **32** (1999) R131.

[120] S. Amoruso, M. Armenante, V. Berardi, R. Bruzzese, N. Spinelli. "*Absorption and saturation mechanisms in aluminum laser ablated plasmas*", Appl. Phys. **A 65** (1997) 265.

[121] J.R Ho, C. P. Grigoropoulos and J. A. C. Humphrey, "*Gas dynamics and radiation heat transfer in the vapor plume produced by pulsed laser irradiation of aluminum*", J. Appl. Phys. **79** (1996) 7205.

[122] A. Vertes, M. De Wolf, P. Juhasz and R. Gijbels, "*Threshold conditions of plasma ignition in laser ionisation mass spectrometry of solids*" Anal. Chem. **61**, (1989) 1029.

[123] R. E. Kidder, "*Interaction of Intense Photon and Electron Beams with Plasmas,*" in Physics of High Energy Density, edited by P. Caldirola and H. Knoepfel (Academic, New York, 1971)306.

[124] A. Caruso, R. Gratton, "*Some properties of the plasmas produced by irradiating light solids by laser pulses*", Plasma Phys. **10** (1968) 867.

[125] J. J. Chang and B. E. Warner, "*Laser-plasma interaction during visible-laser ablation of methods*", Appl. Phys. Lett. **69** (1996) 473.

[126] J. G. Lunney and R. Jordan, "*Pulsed laser ablation of metals*", Appl. Surf. Sci. **127–129** (1998) 941.

[127] K.H. Song and X. Xu, "*Mechanisms of absorption in pulsed excimer laser-induced plasma*", Appl. Phys. **A 65** (1997) 477.

[128] B. Zeldovich Ya and P. Raizer Yu "*Physics of Shock Waves and High Temperature hydrodynamic Phenomena*" New York: Academic, 1967.

[129] Spitzer "*Physics of Fully Ionised Gases*", New York, 1962.

[130] J. Hermann, C.B. Leborgne, I.N. Mihailescu, B. Dubrueil, "*Multistage plasma initiation process by pulsed CO_2 laser irradiation of a Ti sample in an ambient gas (He, Ar, or N_2)*", J. Appl. Phys. **73** (1993) 1091.

[131] R.W. Dreyfus, "*Interpreting laser ablation using cross sections*", Surf. Sci. **283** (1993) 177.

[132] P. E. Dyer, "*Electrical characterisation of plasma generation in KrF laser Cu ablation*", Appl. Phys. Lett. **55** (1989) 1630.

[133] J. S. Lash, R. M. Gilgenbach, H. L. Spindler, "*Ionisation dynamics of iron plumes generated by laser ablation versus a laser-ablation-assisted-plasma discharge ion source*", J. Appl. Phys. **79** (1996) 2287.

[134] A. Lenk, B. Schultrich, T. Witke, "*Diagnostics of laser ablation and laser induced plasmas*", Appl. Surf. Sci. **106** (1996) 473.

[135] R. Tambay, R Singh, R W Thareja , "*Studies on recombining Al-plasma using 1.06, 0.532, 0.355, and 0.266 μm laser radiation*", J. Appl. Phys. **72**, (1992) 1197.

[136] F. Garriele, J. Aubreton, A. Catherinot, "*Monte Carlo simulation of the laser-induced plasma plume expansion under vacuum: Comparison with experiments*", J. Appl. Phys. **83** (1998) 5075.

[137] T. E. Itina, A. A. Katassonov, W. Marine, M. Autric, "*Numerical study of the role of a background gas and system geometry in pulsed laser deposition*", J. Appl. Phys. **83** (1998) 6050.

[138] T. E. Itina, W. Marine, M. Autric, "*Monte Carlo simulation of the effects of elastic collisions and chemical reactions on the angular distributions of the laser ablated particles*", Appl. Surf. Sci. **127–129** (1998) 171.

[139] D. Sibold and H. M. Urbassek, "*Kinetic study of pulsed desorption flows into vacuum*", Phys. Rev. **A 43** (1991) 6722.

[140] R. Kelly and R. W. Dreyfus, "*Reconsidering the mechanisms of laser sputtering with Knudsen-layer formation taken into account*", Nucl. Instrum, Methods **B 32** (1988) 341.

[141] A. Namiki, T. Kawai, K. Ichige, "*Angle-resolved time-of-flight spectra of neutral particles desorbed from laser irradiated CdS*", Surf. Sci. **166** (1986) 129.

[142] F. Danvaloo, E. M. Juengermann, T. J. Lee, C.B. Collins, E. Matthias, "*Mass flow in laser-plasma deposition of carbon under oblique angles of incidence*", Appl. Phys. **A 54** (1992) 369.

[143] B. R. Finke, G. Simon, "*On the gas kinetics of laser-induced evaporation of metals*", J. Phys. D: Appl. Phys. **23** (1990) 67.

[144] M. Hanabusa, "*Unique features of laser ablation*", Mater. Res. Soc. Symp. Proc. **285** (1993) 447.

[145] A. Vertes, R. W. Dreyfus, D. E. Platt, "*Modeling the thermal-to-plasma transitions for Cu photoablation*" IBM J. Res. Develop. **38** (1994) 3.

[146] I. NoorBatcha, R. R. Lucchese and Y. Zeiri, "*Effects of gas-phase collisions on particles rapidly desorbed from surfaces*", Phys. Rev. **B 36** (1987) 4978.

[147] R. Cattolica, F. Robben, L. Talbot and D. R. Willis, "*Translational nonequilibrium in free jet expansions*", Phys. Fluids **17** (1974) 1793.

[148] G Scoles, "*Atomic and Molecular Beam Methods*" Oxford, (ed) 1988.

[149] R. K. Singh, N. Biunno, J. Narajan, "*Microstructural and compositional variations in laser-deposited superconducting thin films*", Appl. Phys. Lett. **53**, (1988) 1013.

[150] C. N. Afonso, R. Serna, F. Catalina, D. Bermejo, "*Good-quality Ge films grown by excimer laser deposition*", Appl. Surf. Sci. **46** (1990) 249.

[151] J. Saenger "*Pulsed Laser Deposition*" ed D. B. Chrisey and G H Hubler, New York, 1994.

[152] R. J. Von Gutfeld, R. W. Dreyfus, "*Electronic probe measurements of pulsed copper ablation at 248nm*", Appl. Phys. Lett. **54** (1989) 1212.

[153] D. B. Geohegan, "*Diagnostics and Characteristics of Laser-Produced Plasmas*" in Pulsed Laser Deposition of Thin Films, D. B. Chrisey and G. K. Hubler (editors), John Wiley & Sons Inc., New York, 1994.

[154] J. C. S. Kools, "*Monte Carlo simulations of the transport of laser-ablated atoms in a diluted gas*", J. Appl. Phys. 74 (1993) 6401.

[155] J. Gonzola, C. N. Afonso. I. Madariaga, "*Expansion dynamics of the plasma produced by laser ablation of $BaTiO_3$ in a gas environment*", J. Appl. Phys. **81** (1997) 951.

[156] J. Neamtu, I. N. Mihailescu, Carmen Ristoscu, J. Hermann, "*Theoretical modelling of phenomena in the pulsed-laser deposition process: Application to Ti targets ablation in low-pressure N_2*", J. Appl. Phys. **86** (1999) 6096.

[157] Schreiner P and Urbassek H M, "*Energy and angular distribution of pulsed-laser desorbed particles: the influence of a hot contribution on a cold desorbing species*", J. Phys. D: Appl. Phys. **30** (1997) 185.

[158] G. Callies, H. Schittenhelm, P. Berger and Hugel H, "*Modeling of the expansion of laser-evaporated matter in argon, helium and nitrogen and the condensation of clusters*", Appl. Surf. Sci. **127–129** (1998) 134.

[159] R. F. Wood, K. R. Chen, D. B. Geohegan, A. A. Puretzky, "*Dynamics of plume propagation, splitting, and nanoparticle formation during pulsed-laser ablation*", Appl. Surf. Sci. **127-129** (1998) 151.

[160] B. Lewis and J. C. Anderson, "*Nucleation and Growth of Thin Films*", Academic Press, New York (1978)

[161] M. Schneider, A. Rahman and I. K. Schuller, "*Role of Relaxation in Epitaxial Growth: A Molecular-Dynamics Study*", Physical Reviews Letters **55**, (1985) 604.

[162] C. R. M. Grovenor, H. T. G. Hentzell and D. A. Smith, "*The development of grain structure during growth of metallic films*", Acta Metallurgica **32**, (1984) 773.

[163] D. M. Mattox, "*Film Deposition Using Accelerated Ions*", Rep. SC-DR-**281**, Sandia Corp. (1963) 63

[164] C. M. Gilmore and J. A. Sprague, "*A molecular dynamics analysis of low energy atom-surface interaction during energetic deposition of silver thin films*" Surface Coatings Technology **51** (1992) 324

[165] D. K. Brice, J. Y. Tsao and S. T. Picraux, "*Partitioning of ion-induced surface and bulk displacements*", Nuclear Instruments and Methods in Physical Research **B 44** (1989) 68.

[166] Y. Lifshitz, S. R. Kasi and J. W. Rabelais, "*Subplantation model for film growth from hyperthermal species: Application to diamond*", Physical Review Letters **62** (1989) 1290

[167] I. N. Mihailescu, E. Gyorgy, "*Pulsed Laser Deposition : An Overview*", 4-th ICO Book "*Trends in Optics and Photonics*" ed. T. Asakura (ICO President) (Springer Series in Optical Science, 1999) 201.

[168] K. Murakami, "*Laser Ablation of Electronic Materials-Basic Mechanisms and Applications*", Eds. E. Fogarassy, S. Lazare (Elsevier 1992) 125.

[169] I.N. Mihailescu, V. S. Teodorescu, E. Gyorgy, C. Ristoscu, R. Cristescu, "*Particulates in pulsed laser deposition: formation mechanisms and possible approaches to their elimination*", SPIE Proceedings **4762** (2002) 64.

[170] P. P. Pronko, S. K. Cutta, J. Squier, J. V. Rudd, D. Du , G. Mourou, "*Machining of sub-micron holes using a femtosecond laser at 800nm*", Opt . Commun **114** (1995) 106.

[171] T. J. Goodwin, V. J. Leppert, S. H. Risbud, I. M. Kennedy, and H. W. H. Lee, "*Synthesis of gallium nitride quantum dots through reactive laser ablation*", Appl. Phys. Lett. **70** (1997) 3122

[172] S. Metev, K. Meteva, "*Nucleation and growth of laser-plasma deposited thin films*", Appl. Surf. Sci. **43** (1989) 402.

[173] E. D'Anna, A. Luches, A. Perrone, S. Acquaviva, R. Alexandrescu, I.N. Mihailescu, J. Zemek and G. Majni, "*Deposition of C-N films by reactive laser ablation*", Appl. Surf. Sci. **106** (1996) 126.

[174] A.P. Caricato, G. Leggieri, A. Luches, A. Perrone, E. Gyorgy, I. N. Mihailescu, M. Popescu, G. Barucca, P. Mengucci, J. Zemek and M. Trchova, "*Characterisation of C-N thin films deposited by reactive excimer laser ablation of graphite targets in nitrogen atmosphere"*, Thin Solid Films **307** (1997) 54.

[175] M. von Allmen and A. Blatter, "*Laser-Beam Interactions with Materials*, Springer-Verlag, Berlin, 1995.

[176] J. Turunen, P. Pääkkönen, M. Kuittinen, P. Laakkonen, J. Simonen, T. Kajava, and M. Kaivola, "*Diffractive shaping of excimer laser beams*", J. Mod. Optics **47** (2000) 2467.

[177] S. Acquaviva M. Fernández, G. Leggieri, A. Luches, M. Martino, A. Perrone, "*Pulsed laser ablation deposition of thin films on large substrates*", Appl. Phys. **A 69** (1999) S471.

[178] G. Dinescu, E. Aldea, M.L. De Giorgi, A. Luches, A. Perrone, and A. Zocco, "*Optical emission spectroscopy of molecular species in plasma induced by laser ablation of carbon in nitrogen*", Appl. Surf. Sci. **127-129** (1998) 697.

[179] J. A. Greer and M. D. Tabat, "*Large-area pulsed laser deposition: Techniques and applications*", J. Vac. Sci. Technol. **A 13** (1995) 1175.

[180] Z. Trajanovic, L. Senapati, R. P. Sharma, and T. Venkatesan, "*Stoichiometry and thickness variation of $YBa_2Cu_3O_{7-x}$ in off-axis pulsed laser deposition*", Appl. Phys. Lett. **66** (1995) 2418.

[181] S. R. Foltyn, R. E. Muenchausen, R. C. Dye, X. D. Wu, L. Luo, and D. W. Cooke, "*Large-area, two-sided superconducting $YBa_2Cu_3O_{7-x}$ films deposited by pulsed laser deposition*," Appl. Phys. Lett. **59** (1991) 1374.

[182] M. Lorenz, H. Hochmuth, D. Natusch, H. Börner, G. Lippold, K. Kreher, and W. Schmitz, "*Large-area double-side pulsed laser deposition of $YBa_2Cu_3O_{7-x}$ thin films on 3-in. Sapphire wafers*," Appl. Phys. Lett. **68** (1996) 3332.

[183] V. F. Vratskikh, Y. N. Drodzov, V. V. Talanov, "*Off-axis pulsed laser deposition of CeO_2 buffer and $YBa_2Cu_3O_{7-}$ thin film on both sides of a sapphire substrate in a one-step process*", Supercond. Sci. Technol. **10** (1997) 766.

[184] R. C. Y. Auyeung, J. S. Horwitz, L. A. Knauss, and D. B. Chrisey, "*In situ pulsed laser deposition of large-area ceramic and multilayer films for applications in industry*," Rev. Sci. Instrum. **68**(1997) 3872.

[185] Y. J. Tian, S. Linzen, F. Schmidl, R. Cihar, and P. Seidel, "*Large-area YBCO films for device fabrication*", Supercond. Sci. Technol. **11** (1998) 59.

[186] J. Montalvo, M. Herrera, R. Castro, and J.L. Pena, "*Memorias del SOMI, XI Congreso de Instrumentacion*", edited by G. Ruiz Botello, Ensenada, B.C., Mexico (1996) 466.

[187] J. A. Greer, M. D. Tabat, and C. Lu, "*Future trends for large-area pulsed laser deposition*", Nucl. Instr. and Meth. in Phys. Res. **B 121**(1997) 357.

[188] P.E. Dyer, A. Issa, P.H. Key, "*Dynamics of excimer laser ablation of superconductors in an oxygen environment*", Appl. Phys. Lett. **57** (1990) 186.

[189] J. Gonzalo, C.N. Afonso, J. Perriere, "*Influence of laser energy density on the plasma expansion dynamics and film stoichiometry during laser ablation of BiSrCaCuO*", J. Appl. Phys. **79** (1996) 8042.

[190] A. Catherinot, *Interaction laser-matériaux, aspects thermiques/non thermiques, photoablation et transport de la matière éjectée*, Ecole thématique du CNRS sur l'ablation, Garchy, France (1996) 219.

[191] J. Hermann, A.L Tohmann, C.Boulner-Leborgne, B. Dubreuil, M.L. De Giorgi, A. Perrone, A.Luches, I.N. Mihailescu, *Plasma diagnostics in pulsed laser TiN layer deposition*, J. Appl. Phys. **77** (1995) 2928.

[192] P. James, M. Anognozzi, J. Tamayo, T. J. McMaster, J. M. Newton and M.J. Miles Langmuir, **17** (2001) 349.

[193] Handbook of Modern Ion Beam Materials Analysis, Editors J.R.Tesmer and M.Nastasi, MRS Pittsburg 1995

[194] J. Ch. Barbé, "*Nanocrystalline titanium oxide electrodes for photovoltaic applications*". J Am.Ceram. Soc. **80** (1997) 3157.

[195] D. S. Ginley C. Bright, "*Transparent conducting oxides*", MRS Bulletin **25** (2000) 15.

[196] G. Phatak, R. Lal, "*Deposition and properties of cadmium oxide films by activated reactive evaporation*", Thin Solid Films **245** (1994) 17.

[197] K.L. Chopra, S. Major, D.K. Pandya, "*Transparent conductors-A status review*", Thin Solid Films **102** (1983) 1.

[198] S. Pizzini, N. Butta, D. Narducci, M. Palladino, "*Thick Film ZnO Resistive Gas Sensors*", J. Electrochem. Soc. **136** (1989) 1945.

[199] C.M. Cardile, A.J. Koplick, R. McPherson, B.O. West, "*^{119}Sn Mössbauer spectroscopic study of cadmium stannate films prepared by dip-coating*", J. Mater. Sci. Lett. **8** (1989) 370.

[200] R. Delong, "*The Coating Process: Requirement to Delivery*"Coating Materials News 10 (2000) 3.

[201] I. Hamberg, C.G. Granqvist, "*Evaporated Sn-doped In_2O_3 films: Basic optical properties and applications to energy-efficient windows*", J. Appl. Phys. **60** (1986) R123.

[202] S.H. Brewer, S. Franzen, I*ndium Tin Oxide Plasma Frequency Dependence on Sheet Resistance and Surface Adlayers Determined by Reflectance FTIR Spectroscopy*, J. Phys. Chem. **B 106** (2002) 12986.

[203] R. G. Gordon, "*Criteria for Choosing Transparent Conductors*", MRS Bullettin. **25** (2000) 52.

[204] J.P. Zheng, H.S. Kwok, "*Low resistivity indium tin oxide films by pulsed laser deposition*", Appl. Phys. Lett. **63** (1993) 1.

[205] J.P. Zheng, H.S. Kwok, "*Preparation of indium tin oxide films at room temperature by pulsed laser deposition*", Thin Solid Films **232** (1993) 99.

[206] C. Coutal, A. Azema, J.-C. Roustan, "*Fabrication and characterisation of ITO thin films deposited by excimer laser evaporation*", Thin Solid Films **288** (1996) 248.

[207] F. Hanus, A. Jadin, L.D. Laude, "*Pulsed laser deposition of high quality ITO thin films*", Appl. Surf. Sci. **96–98** (1996) 807.

[208] J.D. Perkins, M.P. Taylor, M.F.A.M. van Hest, C.W. Teplin, J.L. Alleman, M.S. Dabney, L.M. Gedvilas, B.M. Keyes, B. To, D.W. Readey, A.E. Delahoy, S. Guo and D.S. Ginley, 31st IEEE Photovoltaics Specialists Conference (2005) 1.

[209] H. Kim, A. Pique, J.S. Horswitz, H. Mattoussi, H. Murata, Z. H. Kafafi and D. B. Chrisey, "*Indium tin oxide thin films for organic light-emitting devices*", Appl. Phys. Lett. **74** (1999) 3444.

[210] G.K. Hubler, in: D.B. Crisey, G.K. Hubler,_Eds.*Pulsed Laser Deposition of Thin Films*, Wiley, New, York (1994) 327.

[211] Q.X. Jia, J.P. Zheng, H.S. Kwok, W.A. Anderson, "*Indium tin oxide on InP by pulsed laser deposition*", Thin Solid Films **258** (1995) 260.

[212] M. Martino, A.P. Caricato, M. Fernández, G. Leggieri, A. Jha, M. Ferrari, M Mattarelli, "*Pulsed laser deposition of active waveguides*", Thin Solid Films, **433** (2003) 39.

[213] W. Marine, L. Patrone, B. Luk'yanchuk, M. Sentis, "*Strategy of nanocluster and nanostructure synthesis by conventional pulsed laser ablation*", Appl. Surf. Sci. **154-155** (2000) 345.

[214] B. Thestrup, J. Schou, "*Transparent conducting AZO and ITO films produced by pulsed laser ablation at 355nm*", Appl. Phys. **A 69** (1999) S807.

[215] V. Craciun, D. Craciun, Z. Chen, J. Hwang, R.K.Singh, Mat. Res. Soc. Symp., **617** (2000) J3.13.1.

[216] E. Holmelund, B. Thestrup, J. Schou, N.B. Larsen, M.M. Nielsen, E. Johnson, S. Tougaard, "*Deposition and characterisation of ITO films produced by laser ablation at 355nm*", Applied Physics **A 74** (2002) 147.

[217] Y.Hong Zhang, C. K. Chan, J. F. Porter, and W.Guo, "*Micro-Raman spectroscopic characterisation of nanosized TiO_2 powders prepared by vapor hydrolysis*", J. Mater. Res. **13** (1998)

[218] V.W.H. Baur, *Atomabstände und Bindungswinkel im Brookit, TiO_2,* Acta Crystallogr. **14** (1961) 214.

[219] D.J. Dwer, S. D. Cameron and J. Gland, "*Surface modification of platinum by titanium dioxide overlayers: A case of simple site blocking*", surf Sci. **159** (1985) 430.

[220] M.F. Yan and W.W. Rhodes, "*in Grain Boudaries in Semiconductors"*, edited by H.J.Leamy, G. E. Pike and C.H seager (New York, 1981).

[221] J.Reintjes and M.B. Schultz, "*Photoelastic Constants of Selected Ultrasonic Delay-Line Crystals*", J. Appl.Phys. **39** (1968) 5254.

[222] J.B. Goodenough and J.M. Longo, in Landolt-Bornstein Tabellen, edited by K.H. Hellwege and A. M. hellwege (springer verlag, Berlin) 1970.

[223] J. Tauster, S. C Fung, R.L Garten, *Strong metal-support interactions. Group 8 noble metals supported on titanium dioxide*, J. Am Chem soc **100** (1978) 170.

[224] M. Lottiaux. G. Boulesteix. F. Nihoul. F. Varnier. R. Galindo and E. Pelletier, *Morphology and structure of TiO_2 thin layers vs. thickness and substrate temperature* Thin Solid Films. **170** (1989) 167.

[225] S.B. Desu, *Ultra-thin TiO_2 films by a novel method*, Mater. Sci. Eng. **B 13** (1992) 299.

[226] R. I. Bickley, *In Catalysis; Specialist Periodic Reports*; R. Soc. Chem. **5** (1982) 308.

[227] R.H Tait and R.V kasowski, "*Ultraviolet photoemission and low-energy-electron diffraction studies of TiO_2 (rutile) (001) and (110) surfaces*", Phys. Rev. **B 20** (1979) 5178.

[228] K. Tsutsumi, O. Aita, and K. Ichikawa, **"***X-ray Ti K spectra and band structures of oxides of titanium*", Phys. Rev. **B 15** (1984) 4638.

[229] B.W. Veal and A.P. Paulikas, "*Final-state screening and chemical shifts in photoelectron spectroscopy*", Phys. Rev. **B 31** (1985) 5399.

[230] B. Poumellec, P.J. Durham, and G.Y. Guo*, "Electronic structure and X-ray absorption spectrum of rutile TiO_2*" J. Phys. Conden. Matter **3** (1991) 8195.

[231] K.M Glassford and J.R. Chelikowsky, *Structural and electronic properties of titanium dioxide*, Phys. Rev. **B 46** (1992) 1284.

[232] K.M Glassford and J.R. Chelikowsky, *Electronic structure of TiO_2:Ru*, Phys. Rev. **B 47** (1993) 12550.

[233] D. Vogtenhuber, R. Podloucky, A. Neckel, S. G. Steinemann, and A.J. Freeman, "*Electronic structure and relaxed geometry of the TiO_2 rutile (110) surface*", Phys. Rev. **B 49** (1994) 1309.

[234] Yeung, K.W. Lam, "*A simple chemical vapour deposition method for depositing thin TiO_2 films*", Thin Solid Films **109** (1983) 169.

[235] H.K. Ha, M. Yosimoto, H. Koinuma, B. Moon, H. Ishiwara, "*Open air plasma chemical vapor deposition of highly dielectric amorphous TiO_2 films*", Appl. Phys. Lett. **68** (1996) 2965.

[236] G.S. Brady, H.R. Clauser, Materials Handbook, 13th ed., Mc Graw-Hill, New York, (1991) 849.

[237] J. Augustynki, "*Aspects of Photo-Electrochemical and Surface Behaviour of Titanium IV.Oxide*", Springer, Berlin, 1988.

[238] J. Huusko, V. Lantto, H. Torvelsa, "*TiO_2 thick-film gas sensors and their suitability for NO_x monitoring*", Sens. Actuators **B 16** (1993) 245.

[239] B. Poumellec, J. F. Marucco, and B. Touzelin, **"***X-ray-absorption near-edge structure of titanium and vanadium in (Ti,V)O2 rutile solid solutions***"** Phys. Rev. **B 35** (1987) 2284.

[240] W.D. Brown, W.W. Grannemann, "*C-V characteristics of metal-titanium dioxide-silicon capacitors*"Solid State Electron. **21** (1978) 837.

[241] J.D. Perkins, M.F.A.M. van Hest, C.W. Teplin, J.L. Alleman, M.S. Dabney, L.M. Gedvilas, B.M. Keyes, B. To, and D.S. Ginley M.P. Taylor and D.W. Readey A.E. Delahoy and S. Guo "*Combinatorial Optimization of Transparent Conducting Oxides (TCOs) for PV"* 31stIEEE Photovoltaics Specialists Conference and Exhibition Lake, Florida (2005)

[242] P. Wang, P.; S. M. Zakeeruddin, R. Humphry-Baker, J. E. Moser & M. Grätzel *"Molecular-scale interface engineering of TiO_2 nanocrystals: Improving the efficiency and stability of dye-sensitized solar cells."* Adv. Mater. **15** (2003) 2101.

[243] S. Di Mo and W.Y. Ching, "*Electronic and optical properties of three phases of titanium dioxide: Rutile, anatase, and brookite*", Phys. Rev. **B 51**, 13023 (1995).

[244] H. Berger, H. Ang, and F. Levy, "*Growth and Raman spectroscopic characterisation of TiO_2 anatase single crystals*", J. Cryst. Growth **130** (1993) 108.

[245] H. P. Maruska and A. K. Ghosh, "*Photocatalytic decomposition of water at semiconductor electrodes*", Solar Energy **20** (1978) 443.

[246] H. Tang, K. Prasad, R. Sanjines, P. E. Schmid, and F. Levy, "*Electrical and optical properties of TiO_2 anatase thin films*", J. Appl. Phys. **75** (1994) 2042.

[247] G.S. Devi, T. Hyodo, Y. Shimizu, M. Egashira, "*Synthesis of mesoporous TiO_2-based powders and their gas-sensing properties*", Sens. Actuators **B 87** (2002) 122.

[248] V. Gauthier, S. Bourgeois, P. Sibillot, M. Maglione, M. Sacilotti, "*Growth and characterisation of AP-MOCVD iron doped titanium dioxide thin films*", Thin Solid Films **340** (1999) 175.

[249] M. Stomme, A. Gutarra, G.A. Niklasson, C.G. Granqvist, "*Impedance spectroscopy on lithiated Ti oxide and Ti oxyfluoride thin films*", J. Appl. Phys **79** (1996) 3749.

[250] M.P. Moret, R. Zallen, D.P. Vijay, S.B. Desu, "*Brookite-rich titania films made by pulsed laser deposition*", Thin Solid Films, **366** (2000) 8.

[251] N. Lobstein, E. Millon, A. Hachimi, J.F. Muller,M. Alnot, J.L. Ehrhardt, "*Deposition by laser ablation and characterisation of titanium dioxide films on polyethylene-terephthalate*", Appl. Surf. Sci. **89** (1995) 307.

[252] H.K. Ardakani, "*Electrical and optical properties of in situ "hydrogen-reduced" titanium dioxide thin films deposited by pulsed excimer laser ablation*", Thin Solid Films **248** (1994) 234.

[253] A. Suisalu, J. Aarik, H. Mandar, I. Sildos, "*Spectroscopic study of nanocrystalline TiO2 thin films grown by atomic layer deposition*", Thin Solid Films **336** (1998) 295.

[254] A.K. Sharma, R.K. Thareja, U. Willer, W. Schade, "*Phase transformation in room temperature pulsed laser deposited TiO_2 thin films*", Appl. Surf. Sci. **206** (2003) 137.

[255] R. Paily, A. DasGupta, N. DasGupta, T. Ganguli, L M. Kukreja "*Effect of oxygen pressure and laser fluence during pulsed laser deposition of TiO_2 on MTOS,"* Thin Solid Films **462-463** (2004) 57.

[256] D.G. Syarif, A. Miyashita, T. Yamaki, T. Sumita, Y. Choi, H. Itoh, "*Preparation of anatase and rutile thin films by controlling oxygen partial pressure*", Appl. Surf. Sci. **193** (2002) 287.

[257] J. D. DeLoach, C.R. Aita, *"Thickness-dependent crystallinity of sputter-deposited titania"* J. Vac. Sci. Technol. **A16** (1998) 1963.

[258] M. Terashima, N. Inoue, S. Kashiwabara, R. Fujimoto, "*Photocatalytic TiO_2 thin-films deposited by a pulsed laser deposition technique*", Appl.Surf.Sci. **169-170** (2001) 535.

[259] M. Terashima , N. Inoue, S. Kashiwabara, R. Fujimoto, "*Photocatalytic TiO_2 thin-films deposited by a pulsed laser deposition technique*" Applied surface science **169** (2001) 535.

[260] F. Claeyssens, R. J. Lade, K. N. Rosser, M. N. R. Ashfold, "*Investigations of the plume accompanying pulsed ultraviolet laser ablation of graphite in vacuum*" Journal of Applied Physics **89** (2001) 697.

[261] E. Van de Riet, C.J.C.M. Nilleen, J. Dieleman, "*Reduction of droplet emission and target roughening in laser ablation and deposition of metals*", J. Appl. Phys., **74** (1993) 2008.

[262] F. Claeyssens, R.J. Lade, K.N. Rosser, M.N.R. Ashfold, "*Investigations of the plume accompanying pulsed ultraviolet laser ablation of graphite in vacuum*", J. Appl. Phys. **89** (2001) 697.

[263] A. Shevelko, A. Antonov, I. Grigorieva, Y. Kasyanov, O. Yakushev, L. V. Knight, Q. Wang, "*X-ray focusing crystal von Hamos spectrometer with a CCD linear array as a detector*," in Advances in Laboratory-based X-Ray Sources and Optics; eds.Proc. SPIE **4144** (2000) 148.

[264] R. Dolbec, M.A. El Khakani, A.M. Serventi, M. Trudeau, R.G. Saint-Jacques, "*Microstructure and physical properties of nanostructured tin oxide thin films grown by means of pulsed laser deposition*", Thin Solid Films **419** (2002) 230.

[265] R. Dolbec, M.A. El Khakani, A.M. Serventi, R.G. Saint-Jacques, "*Influence of the nanostructural characteristics on the gas sensing properties of pulsed laser deposited tin oxide thin films*", Sens. Actuators **B 93** (2003) 566.

[266] C.K. Kim, S.M. Choi, I.H. Noh, J.H. Lee, C. Hong, H.B. Chae, G.E. Jang, H.D Park, "*A study on thin film gas sensor based on SnO_2 prepared by pulsed laser deposition method*", Sens. Actuators **B 77** (2001) 463.

[267] W.S. Hu, Z.G. Liu, J.G. Zheng, X.B. Hu, X.L. Guo, W. Göpel, "*Preparation of nanocrystalline SnO_2 thin films used in chemisorption sensors by pulsed laser reactive ablation*", J. Mater. Sci. **8** (1997) 155.

[268] S.Nicoletti, L.Dori, F.Corticelli, M.Leoni, P.Scardi, "*Tin Oxide Thin-Film Sensors for Aromatic Hydrocarbons Detection: Effect of Aging Time on Film Microstructure*" J. Am. Ceram. Soc. **82** (1999) 1201

[269] H. Yumoto, K. Watanabe, K. Akashi, N. Igata, "*The effect of electronic excitation produced by an electron shower on the adhesion of copper films deposited on stainless steel*", Appl. Surf. Sci., **48/49** (1991) 173.

[270] T.K. Yong, T.Y. Tou and B.S. Teo, "*Pulsed laser deposition of tin-doped indium oxide (ITO) on polycarbonate*", Appl. Surf. Sci. **248** (2005) 388.

[271] G. Fang, D. Li and Bao-Lun Yao, "*Magnetron sputtered AZO thin films on commercial ITO glass for application of a very low resistance transparent electrode*", J. Phys. D: Appl. Phys. **35** (2002) 3096.

[272] X. W. Sun, H. C. Huang, and H. S. Kwok, "*On the initial growth of indium tin oxide on glass*", Appl. Phys. Lett. **68** (1996) 2663

[273] C. H. Yi, Y. Shigesato, I. Yasui, S. Takaki, "*Microstructure of Low-Resistivity Tin-Doped Indium Oxide Films Deposited at 150-200°C*", Jpn. J. Appl. Phys. **34** (1995) L244.

[274] A E. Jimenez-Gonzalez, J A. Soto-Urueta and R. Suarez-Parra, "*Optical and electrical characteristics of aluminum-doped ZnO thin films prepared by solgel technique*", J. Cryst. Growth **192** (1998) 430.

[275] JCPDS Card No. 06-0416. Powder Diffraction File, JCPDS International Centre for Diffraction Data, PA, USA, 1995.

[276] D.J. Li, "*Reduction of residual gas in a sputtering system by auxiliary sputter of rare-earth metal*", J. Vac. Sci. Technol. **A 20** (2002) 33.

[277] O. Vigil, F. Cruz, G. Santana, L. Vaillant, A. Morales-Acevedo and G. Contreras-Puente, "*Influence of post-thermal annealing on the properties of sprayed cadmium–zinc oxide thin films*" Appl. Surf. Sci. **161** (2000) 27.

[278] B. D. Cullity "*Elements of X-ray Diffraction*" 2nd edn (Reading, MA: Addison Wesley) (1978) 102.

[279] D. G. Neerinck, T. J. Vink, "*Depth profiling of thin ITO films by grazing incidence X-ray diffraction*", Thin Solid Films **278** (1996) 12.

[280] H. Y. Yeom, N. Popovich, E. Chason, D. C. Paine, "*A study of the effect of process oxygen on stress evolution in D.C. magnetron-deposited tin-doped indium oxide*", Thin Solid Films **411** (2002) 17.

[281] F. O. Adurodija, H. Izumi, T. Ishihara, H. Yoshioka, M. Motoyama, "*Effects of stress on the structure of indium-tin oxide thin films grown by pulsed laser deposition*", J. Mat. Science: Mat. In Electronics **12** (2001) 57.

[282] K.H. Yoon, J.S. Song, "*Properties of fluorine-doped SnO_2 films prepared by the pyrosol deposition method*", Sol. Energy Mater Sol. Cells **28** (1993) 317.

[283] K. Suzuki, N. Hasimoto, T. Oyama, J. Shimizu, Y. Auao, H. Kojima, "*Large scale and low resistance ITO films formed at high deposition rates",* Thin Solid Films **226** (1993) 104.

[284] E. Shanthi, V. Dutta, A. Banerjee, K. Chopra, "*Electrical and optical properties of undoped and antimony-doped tin oxide films*", J. Appl. Phys. **51** (12) (1986) 6243.

[285] I.A. Rauf, "*A comparison of scanning tunnelling microscopy with conventional and scanning transmission electron microscopy using tin-doped indium oxide thin films*", Surf. Sci. 325 (1995) 413.

[286] D.H. Levi, H.R. Moutinho, B.M. Keyes, F.S. Hasoon, R.K. Ahrenkiel, M. Al-Jassim, L.L. Kasmerski, R. Birkmire, "*Micro-Thorough Nanostructure Investigations of Polycrystalline CdTe: Correlations with Processing Electronic Structures*", Solar Energy Material and Solar Cell **41-42**, (1996) 381.

[287] J. A. Dagata, "*Device Fabrication by Scanned Probe Oxidation*", Science **270**, Perspectives Section (1995) 1625.

[288] J. George, K.S. Joseph, B. Pradeep, T.I. Palson, "*Reactively evaporated films of indium sulphide*", Phys. Stat. Sol. **A. 106**, Applied Research (1988) 123.

[289] P.S. Vincett, "*Deposition rate dependence of the critical optimization temperature for thin film properties: Evidence for the disordered area reevaporation mechanism*", J. Vac. Sci. Technol. **21** (1982) 972.

[290] P.S. Vincett, "*Critical optimisation*", Thin Solid Films **100** (1983) 371.

[291] H. Lin, Tetsuro Jin, Andriy Dmytruk, Makoto Saito, Tetsuo Yazawa, "*Preparation of a porous ITO electrode*", J. of Photochem. and Photobiol. A: Chemistry **164** (2004) 173

[292] H. Lin, T. Jin, A. Dmytruk, T. Yazawa, "*Preparation of a Translucent, Conductive, Porous Nanocomposite*", J. Am. Cerm. Soc., **86** (11), (2003) 1991.

[293] N.G. Park, J. van de Lagemaat, A.J. Frank, "*Comparison of Dye-Sensitised Rutile- and Anatase-Based TiO_2 Solar Cells*", J. Phys. Chem. **B 104** (2000) 8989.

[294] I.J. van der Pauw Philips Research Reports, **13(1),** 1 (1958)

[295] Y. Shigesato, S. Takaki, T. Haranoh, "*Crystallinity and electrical properties of tin-doped indium oxide films deposited by DC magnetron sputtering*", Appl. Surf. Sci. **48-49** (1991) 269.

[296] Y. Shigesato, D.C. Paine, "*A microstructural study of low resistivity tin-doped indium oxide prepared by D.C. magnetron sputtering*", Thin Solid Films **238** (1994) 44

[297] R.B.H. Tahar, T. Ban, Y. Ohya, Y. Takahashi, "*Tin doped indium oxide thin films: Electrical properties*", J. Appl. Phys. **83** (1998) 2631.

[298] F.O. Adurodija, H. Izumi, T. Ishihara, H. Yoshioka, K. Yamada, H. Matsui, M. Motoyama, "*Highly conducting indium tin oxide (ITO) thin films deposited by pulsed laser ablation*", Thin Solid Films **350** (1999) 79.

[299] T. Ohsaka,F. Izumi, and Y. Fujiki, "*Raman spectrum of anatase, TiO_2*", J. Raman Spectrosc**. 7,** (1978) 321.

[300] T.V. Nguyen, O.B. Yang, "*Photoresponse and AC impedance characterization of TiO_2–SiO_2 mixed oxide for photocatalytic water decomposition*", Catal. Today **87** (2003) 69.

[301] S. Kelly, F. H. Pollak, and M. Tomkiewicz, "*Raman Spectroscopy as a Morphological Probe for TiO_2 Aerogels*" J. Phys. Chem. **B 101** (1997) 2730.

[302] G. Busca, G. Ramis, J. M. G. Amores, V. S. Escribano, and P. Piaggio, "*FT Raman and FTIR studies of titanias and metatitanate powders*", J. Chem. Soc. Faraday Trans. **90** (1994) 3181.

[303] H. Lin, T. Yoko, M. Takahashi, Japanese Patent, Open No.2001-44469 (1999).

[304] A.L. Linsebigler, G. Lu, J.T. Yates Jr., "*Photocatalysis on TiO_2 Surfaces: Principles, Mechanisms, and Selected Results*", Chem. Rev. **95** (1995) 735.

[305] F. Fotsa Ngaffo, A. P. Caricato, M. Fernandez, M. Martino, F. Romano. "*Structural properties of single and multilayer ITO and TiO_2 films deposited by Reactive pulsed laser*" accepted for publication in the journal of Applied Surface Science, September 2006.

[306] L. Gupta, A. Mansingh, P.K. Srivastava, "*Band gap narrowing and the band structure of tin-doped indium oxide films*", Thin Solid Films **176** (1989) 33.

[307] S. Ray, R. Banerjee, N. Basu, A.K. Batabyal, A.K. Barua, "*Properties of tin doped indium oxide thin films prepared by magnetron sputtering*", J. Appl.Phys. **54** (1983) 3497.

[308] E. Burstein, "*Anomalous Optical Absorption Limit in InSb*", Phys. Rev. **93** (1954) 632.

[309] A. Ben- Shalom, L. Kaplan, R. Boxman, S. Goldsmith, M. Nathan, "*SnO_2 transparent conductor films produced by filtered vacuum arc deposition*", Thin Solid Films **236** (1993) 20.

[310] M. Mizuhashi, "*Electrical properties of vacuum-deposited indium oxide and indium tin oxide films*", Thin Solid Films **70** (1980) 91.

[311] O.S. Heavens, "*Optical Properties of Thin Solid Films*", Dover Publications, New York (1991) 115.

[312] G. Tamizhmani, M. Cocivera, R.T. Oakley, C. Fischer, M.Fujimoto, "*Physical characterisation of a-Si thin films deposited by thermal decomposition of iodosilanes*", J. Phys. D: Appl. Phys. **24** (1991) 1015.

[313] Damodara Das,.Shahil Kirupavathy, Laxmikant Damodare, N. Lakshminarayan, "*Optical and electrical investigations of indium oxide thin films prepared by thermal oxidation of indium thin films*", J. Appl. Phys.**79** (11) (1996) 8521

[314] C. J . Brinker, G. C. Frye, A. J . Hurd, C. S .Ashley, "*Fundamentals of sol-gel dip coating*", Thin Solid Films **201** (1991) 97.

[315] M.M. Yashida, V.C. Martinez, P.A. Madrid, A.A. Elguezabal, "*Thin films of photocatalytic TiO_2 and ZnO deposited inside a tubing by spray pyrolysis*", Thin Solid Films **419** (2002) 60.

[316] M.I.B. Bernardi, E.J.H. Lee, P.N. Lisboa-Filho, E.R. Leite, E.Longo, J.A. Varela "*TiO_2 Thin Film Growth Using the MOCVD*" Method Mater. Res. **4** (2001) 223.

[317] D. Luca, L.S. Hsu, "*structural evolution and optical properties of TiO_2 thin films prepared by thermal oxidation of PLD Ti films*" J. Optoel, Adv. Mater. **5** (2003) 835.

[318] P. Lobl, M. Huppertz, D. Mergel, "*Nucleation and growth in TiO_2 films prepared by sputtering and evaporation*", Thin Solid Films **251** (1994) 72.

[319] K. Fukushima, I. Yamada, "*Surface smoothness and crystalline structure of ICB deposited TiO_2 films*", Appl. Surface Sci. **43** (1989)32.

[320] T. Nishide and F. Mizukami, "*Effect of ligands on crystal structures and optical properties of TiO_2 prepared by sol-gel processes*", Thin Solid Film. **353** (1999) 67.

[321] J. Pascual, J. Camassel, and M. Mathieu, "*Fine structure in the intrinsic absorption edge of TiO_2*", Phys. Rev. **B 18** (1978) 5606.

[322] N. Daude, C. Gout, and C. Jouanin, "*Electronic band structure of titanium dioxide*", Phys. Rev. **B 15**, (1977) 3229.

[323] H. Tang, H. Berger, P. E. Schmid, F. Levy, and G. Burri, "*Photoluminescence in TiO_2 anatase single crystals*", Solid State Commun. **87** (1993) 847.

[324] S. Tanemura, L. Miao, P. Jin, K. Kaneko, A. Terai, and N. Nabatova-Gabain, "*Optical properties of polycrystalline and epitaxial anatase and rutile TiO_2 thin films by rf magnetron sputtering*", Appl. Surf. Sci. **212-213**, (2003) 654.

[325] H. Tomaszewski, H. Poelman, D. Depla, D. Poelman, R. de Gryse, L.Fiermans, M.-F. Reyniers, G. Heynderickx, and G. B. Marin, "*TiO_2 films prepared by DC magnetron sputtering from ceramic targets*", Vacuum **68**, (2003) 31.

[326] N. Martin, C. Rousselot, C. Savall, and F. Palmino, "*Characterisations of titanium oxide films prepared by radio frequency magnetron sputtering*", Thin Solid Films **287** (1996) 154.

[327] F. Fotsa Ngaffo, A. P. Caricato, M. Fernandez, M. Martino, F. Romano. Armando Luches "*Optical properties of ITO/TiO_2 multilayer thin films deposited by RPLAD*" in preparation

[328] F. Fotsa Ngaffo, A. P. Caricato, M. Fernandez, M. Martino, F. Romano. Armando Luches "*Effect of the Au nanoparticles on the optical properties of ITO/TiO_2 multilayer thin films deposited by RPLAD*" in preparation